THE UNIVERSITY OF MANITOBA

DEPARTURES FROM MATTHIESSEN'S RULE IN DILUTE Pd AND Pt BASED ALLOYS

by

ELAHEH K. AZARBAR

A THESIS

SUBMITTED TO THE FACULTY OF GRADUATE STUDIES

IN PARTIAL FULFILMENT OF THE REQUIREMENTS FOR THE DEGREE

OF MASTER OF SCIENCE

DEPARTMENT OF PHYSICS

WINNIPEG, MANITOBA

May, 1975

DEPARTURES FROM MATTHIESSEN'S RULE IN DILUTE Pd AND Pt BASED ALLOYS

by

ELAHEH K. AZARBAR

A dissertation submitted to the Faculty of Graduate Studies of the University of Manitoba in partial fulfillment of the requirements of the degree of

MASTER OF SCIENCE

ABSTRACT

The electrical resistivity of several dilute Pd and Pt based alloys containing between 0.1 and 1.0 at % Ti has been measured over a range from 4.2K to room temperature.

These alloys show departures from Matthiessen's Rule which can be explained by a (K.S.W.) equation:

$$\frac{1}{\Delta(T)} = \frac{1}{\beta\rho_o} + \frac{1}{\gamma\ \rho_{ph}}$$

The two band model which has been used to explain the behaviour of noble metal alloys can also explain the data obtained with platinum and paladium alloys, but, since the electronic band structure is quite different in Pt and Pd and Au, the physical basis for this behaviour is unclear.

Specifically, the experimental results have been explained on the basis of the two band model with constant β and temperature-dependent γ in Pt Ti and Pt V alloys and temperature-dependent β and γ in the case of Pd Ti alloys.

The values of α_p (the ratio of the conductivity of the two "sets" of carriers when the scattering is due to phonons) initially increases smoothly with temperature, but at higher temperatures this trend is reversed and α_p decreases with increasing temperature. This change in the temperature derivative of α_p occurs near the transition $\gamma > \beta$ to $\beta > \gamma$.

ACKNOWLEDGEMENTS

I am greatly indebted to Dr. Gwyn Williams under whose supervision this study was carried out. His suggestions and encouragements throughout this work are highly appreciated.

Thanks are also due to Mrs. Betty Glowasky for the excellent job she has done in typing the manuscript.

TABLE OF CONTENTS

CHAPTER ONE

THEORETICAL CONCEPTS

INTRODUCTION

An electron can move quite freely through a perfect lattice, which would consequently have no resistance. The resistance of a pure metal is due to the thermal agitation of the atoms, which destroys the periodicity of the lattice. When, moreover, a foreign atom is present in solid solution, the periodicity of the field within the lattice is broken at that point. This effect may be considered not to affect the zone structure very much in the case when a small amount of metal has been dissolved in a metallic host (dilute alloys), and the resulting alloy has the same crystal structure as the host. Electrons may be deflected by that atom and a resistance will arise, even in the absence of any temperature induced agitation.

Some of the earliest investigations in this area are due to Matthiessen[1] who noted that the temperature dependence of the resistivity in the dilute alloy was the same as in the host. He thus deduced that the impurity resistivity $\rho_i(C,0)$ is independent of temperature, and wrote $\rho_a(C,T)$ (resistivity of a dilute alloy containing a concentration C of impurity), as:

$$\rho_a(C,T) = \rho_p(T) + \rho_i(C,0) \qquad (1\text{-}1)$$

where $\rho_a(T)$ is resistivity of ideally pure metal. Equation (1-1) has become known as Matthiessen's Rule (MR).

After Matthiessen, measurements were extended to lower temperatures and it was found out that MR does not apply at these temperatures.

In order to get the correct result, a term $\Delta(C,T)$ should be added to equation (1-1).

$$\rho_a(C,T) = \rho_p(T) + \rho_i(C,0) + \Delta(C,T) \qquad (1\text{-}2)$$

$\Delta(C,T)$ depends both on temperature and impurity concentration. Even in alloys where $\rho_i(C,0)$ is independent of temperature, it is still possible to observe a temperature dependent $\Delta(C,T)$. The origins of this effect will be discussed later.

In addition, when the impurity has an internal structure, such as a magnetic moment, then the impurity contribution to the resistivity is itself temperature dependent, leading to a temperature dependent $\Delta(C,T)$ as described by equation (1-2).

The major source of resistivity in metals is scattering of conduction electrons by phonons, which is temperature dependent. Magnetic impurities can cause a deviation $\Delta(C,T)$ which often appears as a minimum in the resistivity at very low temperatures[2]. This effect has been explained by Kondo[3] as an interaction between conduction electron pairs coupled by spin flipping due to the impurity magnetic moment.

If a dilute alloy is made by dissolving a first row transition atom impurity in a simple metal, it is often found that the impurity atom possesses a net magnetic moment. The formation of these local moments are due to the presence of virtual-bound-states at the impurity site (for a review see (2)). Frequently, due to the finite lifetime of a virtual-bound-state, which may be regarded as rapid changes in orientation of the localized moment, measurement of properties such as susceptibility which are a "long time" average reveal no observable moment due to this rapid spin flipping. However, these fluctuations in the localized spin will scatter conduction electrons provided the spin

fluctuation lifetime, ($\tau_{sf} = \frac{\hbar}{k_B\theta}$) where θ is ℓsf temperature, is greater than the thermal fluctuation lifetime $\tau_{thermal} = \frac{\hbar}{k_B T}$ of the conduction electrons. Otherwise, the conduction electron does not "see" a magnetic moment and no magnetic scattering exists.

In recent years the description of the behaviour of first-row transition metals from Cr to Ni in Pd and other hosts has been received considerable attention, with the current consensus of opinion being that there are localized spin fluctuating (ℓsf) systems.

Kaiser and Doniach[4] have derived an expression for the scattering of conduction electrons from localized spin fluctuation, which, when potential (coulomb) scattering is included yields the following form for the incremental resistivity $\Delta\rho(T)$:

$$\frac{\Delta\rho(T)}{C} = A + B \ \ell n \ [(T^2 + \theta^2)^{\frac{1}{2}}] \qquad (1\text{-}3)$$

here θ is ℓsf characteristic temperature (Tsf) and A and B are constants.

The phase shift model[5] which yields

$$B \propto \cos\left(\frac{\pi z}{(2\ \ell+1)}\right) \qquad (1\text{-}4)$$

where z is the effective host-impurity charge difference and $(2\ell+1)$ the orbital degeneracy of the state considered (5 for d electrons), predicts the correct sign for B in alloys of the first row transition metal impurities in Pd (and other hosts).

The ℓsf temperatures and the sign of B (which determines $\Delta\rho(T)$ increases or decreases with increasing temperature) are shown in table (1-1)

Impurity	Sign of B	$T_s(\theta)$ (host Pd)	$T_s(\theta)$ (host Pt)
Ni	+	~80[4]	10^2-10^3[6]
Co	+	< 1[7]	~1[8]
Fe	+	<< 1[8]	0.1-1[5] 0.4 K
Mn	-	<< 1	<< 1[9]
Cr	-	~30[10]	~60[11]
V	-	~160[12]	> 10^3
Ti	-	> 10^3	> 10^3

TABLE (1-1)

From this table it can be seen that the ℓsf temperatures for Pt V, Pd T_i and Pt T_i are high, so that there should be little contribution to $\Delta\rho(T)$ (and hence $\Delta(T)$) from conduction electrons scattering from ℓsf, at least at temperatures below room temperature. These latter alloys thus appear as prime candidate for the observation of conventional MR deviations (DMR), uncomplicated by the presence of "magnetic" scattering.

Historical Background

About 110 years ago, A. Matthiessen and C. Vogt carried out some measurements on the resistivity of a series of dilute alloys between ice point and the boiling point of water.

They found that the temperature derivative of the resistivity $\rho_p(T)$ of an ideally pure metal could be approximated by this relation:

$$\frac{d\,\rho_a(C,T)}{dT} = \frac{d\,\rho_p(T)}{dT} \qquad (1\text{-}5)$$

where $\rho_a(C,T)$ is the resistivity of a dilute alloy containing a concentration C of impurity.

If equation (1-5) applies exactly at all temperatures, by integrating it we can obtain equation (1-1) which is known as Matthiessen's Rule.

We can show $\rho_i(C,0)$, the impurity produced resistivity at 0°K by $\rho_o(C)$.

The major source of resistance is the vibrations of the lattice ions themselves due to their thermal energy, and is termed the ideal or phonon resistivity. It vanishes at $T = o$, and is the same for all specimens of a particular metal and alloys having that metal as major constituent.

The other source of scattering is static lattice defects, such as impurities, vacancies and dislocation, which gives rise to a residual resistivity and vanishes for an ideally pure and structurally perfect metal. This part of resistance is due to the breakdown in the periodicity of the potential in the lattice, which may be due to two causes:

1) the impurity atom may distort the lattice and push the neighbouring atoms out of position (lattice distortion).
2) the field within the impurity unit cell will be different from that within a host atom unit cell, so scattering results from this difference in potential between these two unit cells.

Matthiessen's Rule assumes that the scattering of conduction electrons by phonons and by impurities is independent of each other and that effectively a single relaxation time can characterize each type of scattering.

In practice there are always deviations from Matthiessen's Rule,

(DMR).

However, in many cases these deviations are small compared to either $\rho_p(T)$ or to $\rho_o(C)$ or to both, and MR represents quite a good approximation to the experimental data.

The deviations from MR can only be significant when the ideal and impurity induced resistances are of the same order of magnitude.

The resistivity of an alloy can be written exactly as equation (1-2):

$$\rho_a(C,T) = \rho_p(T) + \rho_o(C) + \Delta(C,T) \qquad (1\text{-}2)$$

where $\Delta(C,T)$ is the deviation from MR and depends on the nature and concentration of defects and impurities, as well as temperature.

The variation of $\frac{d\,\rho_a(C,T)}{dT}$ with impurity concentration is approximately linear at low concentration, and sometimes $\frac{d\,\rho_a(C,T)}{dT}$ decreases upon the addition of certain transition metal impurities.

Major points in the observed behaviour of $\Delta(C,T)$

The early measurements of the deviations from MR established that $\Delta(C,T)$ is positive and rises from a low temperature plateau (the residual resistance when phonon scattering is negligible) to a higher value (when phonon scattering is dominant).

At these latter temperatures, $\Delta(C,T)$ usually consists of a constant term and a term varying approximately linearly with temperature. Both terms usually vary approximately linearly with concentration.

At intermediate temperatures $\Delta(C,T)$ may contain a hump, particularly in dilute alloys. This hump increases in relative magnitude and moves toward lower temperatures as the impurity content decreases.

Figure (1-1) shows the typical variation of $\Delta(C,T)$ with temperature[13].

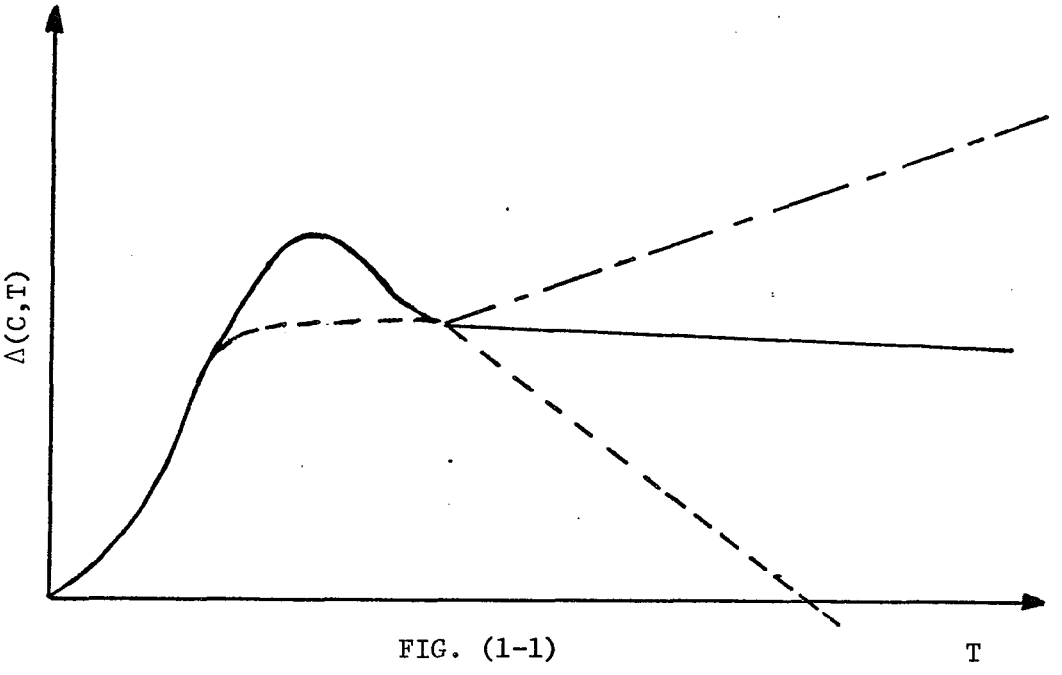

FIG. (1-1)

The major qualitative features of the experimentally observed temperature deviation of $\Delta(C,T)$. The different curves represent different possible forms of $\Delta(C,T)$.

Deviations from Matthiessen's Rule, DMR, can arise theoretically for a number of reasons.

Some of the most important ones (for non-magnetic impurities) are as follows:

1) changes in the electronic band structure, (Fermi surface)
2) the introduction of an impurity atom into a lattice can change the vibrational characteristics of the lattice, and hence, phonon spectrum. This means that the θ_D value of the lattice is altered
3) the phonon distribution may be perturbed by the added impurity

4) scattering processes which involve phonons and impurities simultaneously, and are included neither in $\rho_p(T)$ nor in $\rho_o(C)$, (phonon-assisted impurity scattering)

5) the relaxation times for phonon and impurity scattering may have different anisotropies.

Other causes are boundary size effect at low temperatures, phonon drag and changes in the atomic volume upon alloying.

Some of these contributions are small and negligible while there are others whose contributions are rather difficult to estimate. In particular, numbers (1) and (4) are very difficult to estimate, while (5) can only be treated phenomenogically (Viz, by fitting the observed $\Delta(C,T)$ to the predicted form arising from such anisotropies).

In the case of (2) and (3), Kagan and Zhernov[14] have given a thoery for deformation of the phonon spectrum due to the introduction of impurity atoms and also the change in the scattering potential at the site of the impurity. While first principle calculations of such effects in the present system are quite difficult to perform, we note that in the CuSn system[15] (where the impurity-host mass ratio is not greatly different from that in the present alloys) the estimated correction from this source was about 0.05 $\mu\Omega$ cm between 90 and 300K. This correction is no larger than shape factor uncertainties (discussed later) and hence its neglect should not affect subsequent conclusions.

In addition to the above, thermal effects usually give rise to small contributions to DMR, and these may be discussed under the following headings:

(i) changes in the geometrical form factor (i,e, the area to length ratio for the sample). The magnitude of this depends

on thermal expansion of the alloy. For Pt based alloys it amounts to 0.016 and for Pd based alloys amounts to 0.020.

(ii) changes in the atomic volume of the lattice produced both thermally and as a result of alloying should be taken into account. Dugdale and Basinski[16] have pointed out that one should only attempt to apply Matthiessen's Rule, when ρ_{total}, ρ_{phonon} and ρ_o are measured at the same atomic volume.

a) thermal changes in the atomic volume produce changes in the impurity "residual" resistivity ρ_o, which are temperature dependent. This correction has the form:

$$3\,\alpha\,\rho_o\left(\frac{d(\ell n\ \rho_o)}{d(\ell n\ V)}\right)T \qquad (1\text{-}6)$$

where α is the coefficient of linear expansion. Estimates for $\frac{d(\ell n\ \rho_o)}{d(\ell n\ V)}$ are difficult to obtain, but taking a value of -0.5 (as deduced from Bridgmann's[17] data for Si in Fe) as "typical", we obtain a contribution of about $-5\rho_o \times 10^{-3}$ from this source, which amounts to less than -0.02 μΩ cm and is generally considerably smaller than shape factor uncertainties in the alloys considered here.

b) the ideal resistivity of the pure lattice differs from that in a lattice which is expanded on alloying. Schwerer et al[18] have obtained the following expansion for the contribution to $\Delta(C,T)$ from this source, viz:

$$\frac{3C}{a}\,\rho_{phonon}(T)\left(\frac{d(\ell n\ \rho_{phonon})}{d(\ell n\ V)}\right)\left(\frac{da}{dc}\right) \qquad (1\text{-}7)$$

where a is the lattice spacing.

Using the following values for $\frac{3c}{a} \cdot \frac{da}{dc}$:

0.00036 Per at % in Pd Ti [19]

0.00035 Per at % in Pt Ti

0.00068 Per at % in Pt V

(For PdV we found the value 0.0009[19] for $\frac{da}{dc}$ and used that for PtV) and using the value[17] of

$$\left(\frac{d(\ell n\ \rho_{phonon})}{d(\ell n\ V)}\right) = 4$$

(for the transition metal Fe at room temperature) leads to a contribution of:

0.00144 $\rho_{phonon}(T)$ Per at % in Pd Ti

0.00140 $\rho_{phonon}(T)$ Per at % in Pt Ti

0.00272 $\rho_{phonon}(T)$ Per at % in Pt V

which we consequently neglect.

From the above list of sources of DMR, the following paragraphs outline the origins of deviations from MR suggested by various authors from their observations on different systems.

The change in Debye temperature with alloying (in Magnesium with Aℓ, Ag, Li, Cd) has been suggested as the cause of DMR by Hedgcock and Muir[20] and by Gerritsen and Das[21] (in Magnesium with Lithium, silver, cadmium or tin).

Huebener[22] has shown that there is a small contribution to deviation from Matthiessen's Rule caused by phonon drag effects. The contribution to DMR from phonon drag has a peak at low temperatures. The

calculated size of phonon drag effect is one to two orders of magnitude smaller than the actually observed peak in deviations from Matthiessen's Rule.

Dugdale and Basinski[16] and Matsuda[23] have used the two band model in dilute alloys.

Damon, Mathur and Klemens[24] divided the deviations from MR in dilute gold alloys containing Pt, Cu and In solutes into a two band model and a term approximately proportional to T^4, resulting from the deformation of the impurity potential due to the strain of the lattice in the neighbourhood of the impurity.

Above 20K, only the two band effect seems to be important.

To calculate $\Delta(C,T)$ from first principles it is necessary to calculate the resistivities of both the dilute alloy and the pure host metal, and to determine each of these, it is necessary to attempt a full solution of the Boltzmann equation.

In the present alloy system the contributions from various sources other than the two band model appear to be smaller (at least in these cases where we were able to obtain numerical estimates) than shape factor uncertainties. In these systems then the two band model appears the prime candidate for DMR and consequently a detailed discussion of this model is given below.

Two band model

Matthiessen's Rule is a direct consequence of the existence of isotropic relaxation times for the scattering of electrons by both impurities and phonons, provided that the addition of impurities does not change the properties of electrons and phonons in the pure solvent. But,

because of the essentially anisotropic zone structure, and the importance of Umklapp Processes in the high temperature electrical resistivity, the relaxation time of electrons at the Fermi surface is anisotropic.

The first investigation of the effects on deviations from Matthiessen's Rule of anisotropic scattering was made by Sondheimer and Wilson[25]. They derived a function having the general behaviour of $\Delta(C,T)$ [which increases with temperature and then saturates and increases with solute concentration].

On the presumption that two bands, s and d, contribute to the conductivity, they attributed DMR to the anisotropies of the relaxation times associated with the neck and belly electrons, which may be considered to be equivalent to different bands.

Following Ziman[26], the belly electrons are associated with the more or less spherical parts of the Fermi surface and have something of the character of free electrons. The neck electrons are those associated with the regions of the Fermi surface which are in contact with or close to the {111} Brillouin zone boundaries. Their wave functions can be described by at least two plane waves, which, more exactly, should be orthogonalized (OPW's). Thoery shows that these wavefunctions have their greatest amplitude between the ions (P-like symmetry). P-like electrons tend to move along the channels between the ions.

In considering phonon scattering Ziman used first-order perturbation theory, so that the effect on a mixed wave can be expressed as a matrix element combining contributions from the separate simple plane waves. He concluded that the belly electrons will have a relaxation time τ_B which will tend to increase rapidly at low temperatures, since, Umklapp processes will die out with falling temperature. The relaxation time

of the neck electrons τ_N will not increase so rapidly, because in the neck regions of Fermi surface there is no lower limit to q (phonon wave vector) and Umklapp processes contribute down to the lowest temperatures, so, quite small phonons can still cause appreciable changes in the electron velocity.

Ziman distinguishes between charged and uncharged impurities. Charged impurities are those which do not have the same valency as the parent metal. The scattering from strongly charged impurities tends to be more isotropic and to have τ larger on the bellies than on the necks.

Uncharged impurities are those with the same valence as the host metal, which perturb the lattice potential over a comparatively short range. We expect the scattering of a single plane wave (OPW, actually) to be equivalent to the scattering by a very localized perturbation, (almost a delta function). Such scattering is well known to be s-like. The neck electrons would be scarcely scattered by these impurities because they are in pure P-states, so their relaxation time will be very long.

On the other hand the belly electrons are scattered in the usual way so that $\frac{\tau_N}{\tau_B}$ is large in this case.

At high temperatures phonons have large wave numbers and the scattering will be more or less isotropic, i.e., $\frac{\tau_N}{\tau_B} \approx 1$.

At low temperatures, phonon scattering and impurity scattering may produce very different anisotropies in τ. Thus in an alloy at a temperature where both scattering mechanisms are present, we expect that MR will not be obeyed.

The two band model can be represented schematically by the

following "circuit".

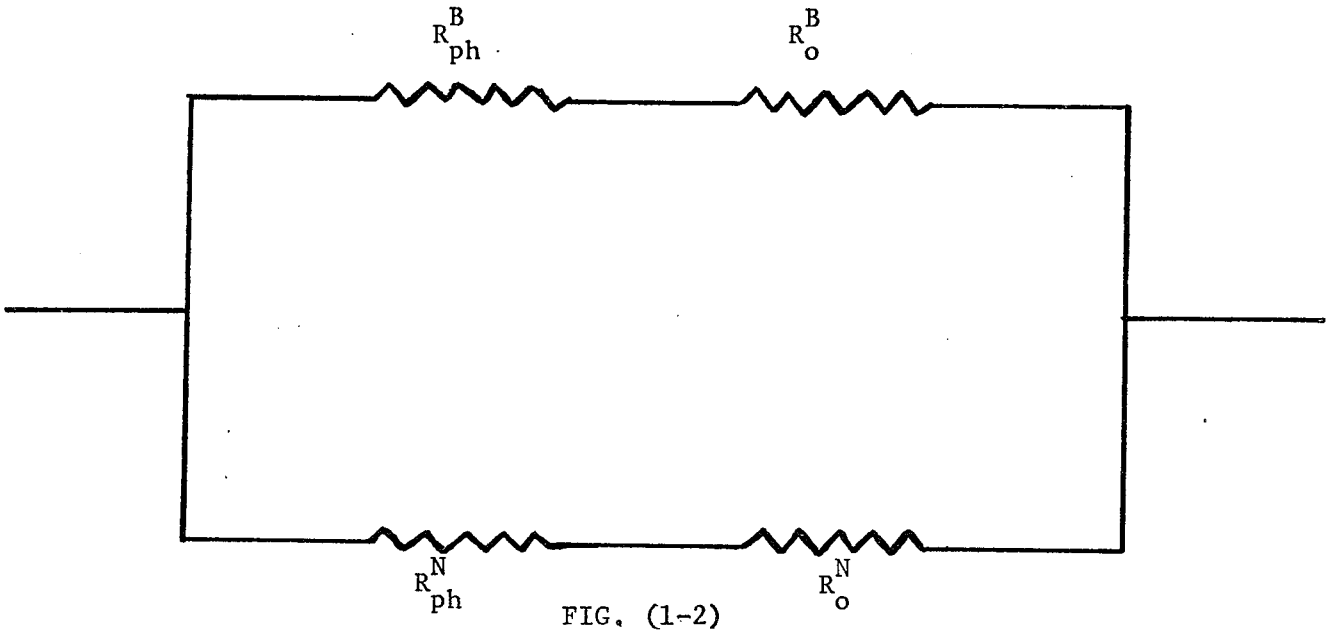

FIG. (1-2)

If the electrons in the two bands do not interact with each other, their conductivities will add and using the standard rules for evaluating the resistance of a series-parallel combination yields the two-band formula.

We call the conductivities of belly and neck electrons σ_B and σ_N, respectively.

The ratio $\frac{\sigma_N \text{ Ph}}{\sigma_B \text{ Ph}}$, the neck to belly conductivities when the scattering is due to phonon alone, will be called α_p and the same quantity when the scattering is due to impurities alone will be called $\alpha_i = \frac{\sigma_N{}^o}{\sigma_B{}^o}$.

From the circuit in Fig. (1-2) we conclude:

$$\rho_{tot} = \frac{(\rho_B^{ph} + \rho_B^o)\ (\rho_N^{ph} + \rho_N^o)}{\rho_B^{ph} + \rho_B^o + \rho_N^{ph} + \rho_N^o} \qquad (1\text{-}8)$$

After some manipulation (Appendix -1), we get:

$$\Delta(C,T) = \frac{\rho_o \rho_{ph}}{\rho_o \frac{\alpha_p(1+\alpha_i)^2}{(\alpha_p - \alpha_i)^2} + \rho_{ph} \frac{\alpha_i(1+\alpha_p)^2}{(\alpha_p - \alpha_i)^2}} \tag{1-9}$$

we call:

$$\gamma = \frac{1}{\alpha_p} \left(\frac{\alpha_p - \alpha_i}{1+\alpha_i}\right)^2 \tag{1-10}$$

and

$$\beta = \frac{1}{\alpha_i} \left(\frac{\alpha_p - \alpha_i}{1+\alpha_p}\right)^2 \tag{1-11}$$

so, we get:

$$\Delta(C,T) = \frac{\gamma\beta \rho_o \rho_{ph}}{\gamma \rho_{ph} + \beta \rho_o} \tag{1-12}$$

and:

$$\frac{1}{\Delta(C,T)} = \frac{1}{\beta \rho_o} + \frac{1}{\gamma \rho_{ph}} \tag{1-13}$$

γ and β can be found by fitting the experimental $\Delta(T)$ curves with this equation. γ and β are positive parameters which are in general different for different solutes and may vary with temperature, therefore in this model $\Delta(C,T)$ must be strictly positive.

Kohler[27] derived an expression for $\Delta(T)$ of precisely the same form as (1-13), but based on different and more general premises. Kohler found the solution of the Boltzmann equation under the applied external field for the case of two simultaneous collision operators representing the impurity scattering and the thermal lattice scattering, respectively, by using the Ritz variational method together with trial distribution functions which solve the problem exactly when the collision operators

act separately. The resulting total resistivity exceeds the sum of the contributions of each operator acting alone, yielding a deviation from Matthiessen's Rule of the form of equation (1-13).

The equation (1-13) is called Kohler-Sondheimer-Wilson (KSW) equation.

This takes a simpler form in two special cases:

i) In the limit:

$$\rho_p(T) << \rho_o(C)$$

$\Delta(C,T)$ will be proportional to $\rho_p(T)$ and independent of $\rho_o(C)$.

ii) In the limit:

$$\rho_p(T) >> \rho_o(C)$$

$\Delta(C,T)$ is proportional to $\rho_o(C)$ and independent of $\rho_p(T)$.

If the parameters γ and β are independent of temperature (as is Sondheimer and Wilson model), $\Delta(C,T)$ will increase monotonically with increasing temperature and at high temperatures will become constant, Fig. (1-3).

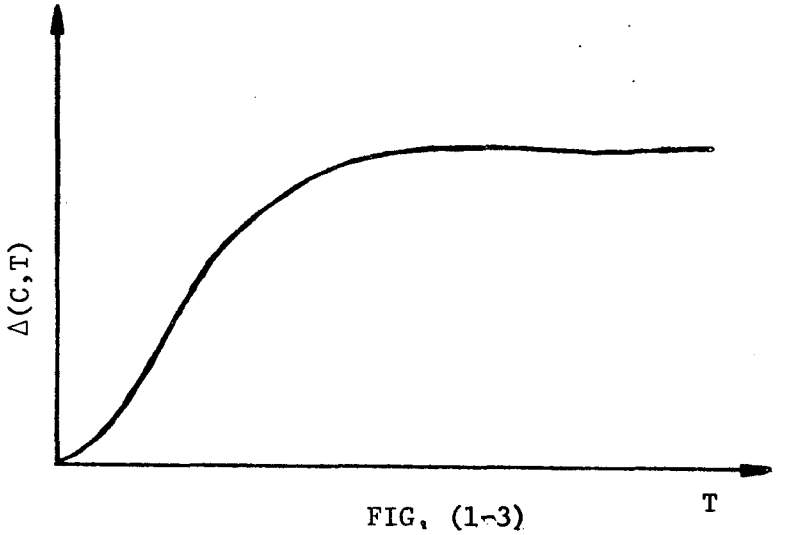

FIG. (1-3)

Variation of $\Delta(C,T)$ with temperature.

If either γ or β varies with temperature, $\Delta(C,T)$ can have quite a different shape. For example it is possible to obtain a hump in $\Delta(C,T)$.

So equation (1-13) is able to describe a large portion of existing data, at least where $\Delta(C,T)$ is positive.

Parameters α_i and α_p can be found by inverting equations (1-10) and (1-11). They yield:

$$\alpha_i = 1 + \frac{1}{2} a \pm \frac{1}{2} a \left(1 + \frac{4}{a}\right)^{\frac{1}{2}} \tag{1-14}$$

$$\alpha_p = 1 + \frac{1}{2} b \pm \frac{1}{2} b \left(1 + \frac{4}{b}\right)^{\frac{1}{2}} \tag{1-15}$$

where:

$$a \equiv \frac{(\gamma - \beta - \gamma\beta)^2}{\gamma^2\beta} \tag{1-16}$$

and:

$$b \equiv \frac{(\beta - \gamma - \beta\gamma)^2}{\gamma\beta^2} \tag{1-17}$$

which then allow information regarding the anisotropy of the scattering to be inferred.

References

1. A. Matthiessen and C. Vogt, Ann. Phys. LPZg, 122, 19, (1864).
2. A.J. Heeger, Solid State Physics, Volume 23, page 283, edited by F. Seitz, D. Turnbull and H. Ehrenreich, Academic Press, New York, (1969).
3. J. Kondo, as in ref. 2, page 183.
4. A.B. Kaiser and S. Doniach, Intern. J. Magnetism, 1, 11, (1970).
5. J.W. Loram, R.J. White and A.D.C. Grassie, Phys. Rev. B5, 3659, (1972).
6. C.A. Mackleit, A.I. Schindler and D. Gillespie, Phys. Rev., B1, 3883, (1970).
7. J.W. Loram, Gwyn Williams and G.A. Swallow, Phys. Rev. B3, 3060, (1971).
8. Gwyn Williams, G.A. Swallow and J.W. Loram, Phys. Rev. B11, 344, (1975).
9. B.V.B. Sarkissian and R.H. Taylor, J. Phys. F: Metal Phys., Vol. 4, L243, (1974).
10. F.C.C. Kao and Gwyn Williams, Phys. Rev., B7, 267, (1973).
11. R.M. Roshko and Gwyn Williams, Phys. Rev., B9, 4945, (1974).
12. F.C.C. Kao, M.E. Colp and Gwyn Williams, Phys. Rev., B8, 1228, (1973).
13. J. Bass, Adv. Phys., 21, 431, (1972).
14. Y. Kagan and A.P. Zhernov, A.P., Zh. eksp. teor. Fiz. 50, 1107-23, (Sov. Phys. JETP, 23, 737-47), (1966).
15. J.O. Linde, Ann. Phys. 15, 219-48, (1932).
16. J.S. Dugdale and Z.S. Basinski, Phys. Rev. 157, 552-60, (1967).

17. P.W. Bridgman, Proc. Am. Acad. Sci., 84, 131, (1955).

18. F.C. Schwerer, J.W. Conroy and S. Arajs, J. Phys. Chem. Solids, 30, 1513-25, (1969).

19. W.B. Pearson, "A handbook of Lattice spacings and structures of metals and alloys", Pergamon Press, (1958).

20. F.T. Hedgcock and W.B. Muir, Phys. Rev., 136, A561, (1964).

21. S.B. Das and A.N. Gerritsen, Phys. Rev., 135, A1081, (1964).

22. R.P. Huebener, Phys. Rev., 146, 502, (1966).

23. Takeshi Matsuda, J. Phys. Chem. Solids, 30, 859, (1969).

24. D.H. Damon, M.P. Mathur and P.G. Klemens, Phys. Rev., 176, 876, (1968).

25. E.H. Sondheimer and A.H. Wilson, Proc. Roy. Soc. (London), 190, 435, (1947).

26. J.M. Ziman, Phys. Rev., 121, 1320, (1961).

27. M. Kohler, Z. Physik, 126, 495, (1949).

CHAPTER TWO

EXPERIMENTAL METHODS

General Description

A four probe method[1] was used to find the resistance of a sample, which was calculated simply from a measurement of the voltage drop produced by a known current across each sample.

In the present arrangement usually six specimens, one pure and five alloys, were mounted in thermal contact with a high conductivity copper block, each of them was clamped on a pair of knife-edge supports (which served as the voltage contacts) located near opposite ends of the block, about 8 cm. apart. These supports were electrically insulated from the block with layers of condenser paper and G.E. varnish.

The voltage tap-off connections were provided by wires, attached to the base of each knife-edge support.

Complete details of the sample mounting block are contained in reference (2).

The samples were series connected current-wise usually using short pieces of copper wire soldered with Woods Metal to the ends of each sample, and the end points of the series were connected to the current supply leads.

At high temperatures, where the resistance is strongly temperature dependent (because of phonon scattering), small differences in temperature between the specimens can lead to significant errors in the differences $\Delta\rho$ between the alloy and the pure-metal resistivities. This source of error is minimized here, as the specimens are held in a constant temperature enclosure in which temperature inhomogenities are not expected to exceed a few millidegrees.

With the apparatus placed in a suitable temperature bath, the heater, wound around the sample block, was used to obtain and regulate

temperatures about 4.2K, and the precise measurements were made with a nonlinear gas thermometer (the uncertainty in the temperature was less than 0.5% of the temperature).

For temperature sensing, a 100Ω Allen-Bradley carbon resistor was mounted on the specimen block and in thermal contact with it. The temperature dependence of the resistance is roughly logarithmic, increasing with decreasing temperature. The approximate temperature points were selected from the characteristic graph of this resistor.

The Allen-Bradley resistor formed one branch of an a-c Wheatstone bridge, Fig. (2-1). This bridge was used for controlling the temperatures of the samples. A resistance box in another arm of the bridge together with carbon resistor characteristic curve were used for dialing an approximate temperature.

A phase sensitive detector supplied a d-c feedback current to the heater to obtain regulated temperatures up to 25K.

Above this point a Heathkit power supply was series-connected to the bridge output permitting temperatures up to room temperature to be obtained.

Electronics:

As already mentioned the standard four-probe technique was used to measure the resistance of the samples at a particular temperature, Fig. (2-2).

A Guildline constant current supply (model 9770B) was used to produce a highly stable current (stable to 1 part in 10^6) through the samples.

The voltage produced by the current across an 0.10Ω Guildline

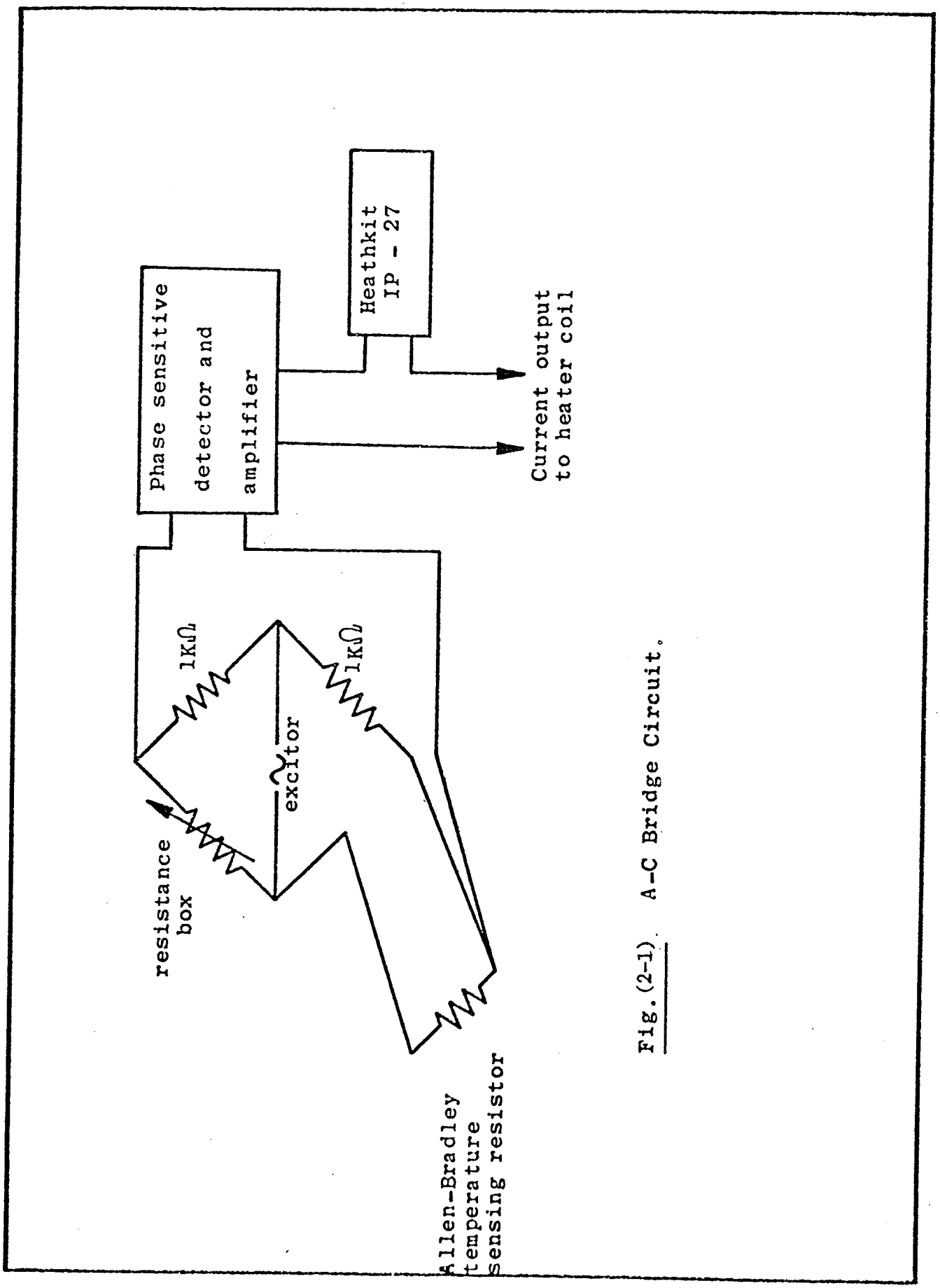

Fig.(2-1). A-C Bridge Circuit.

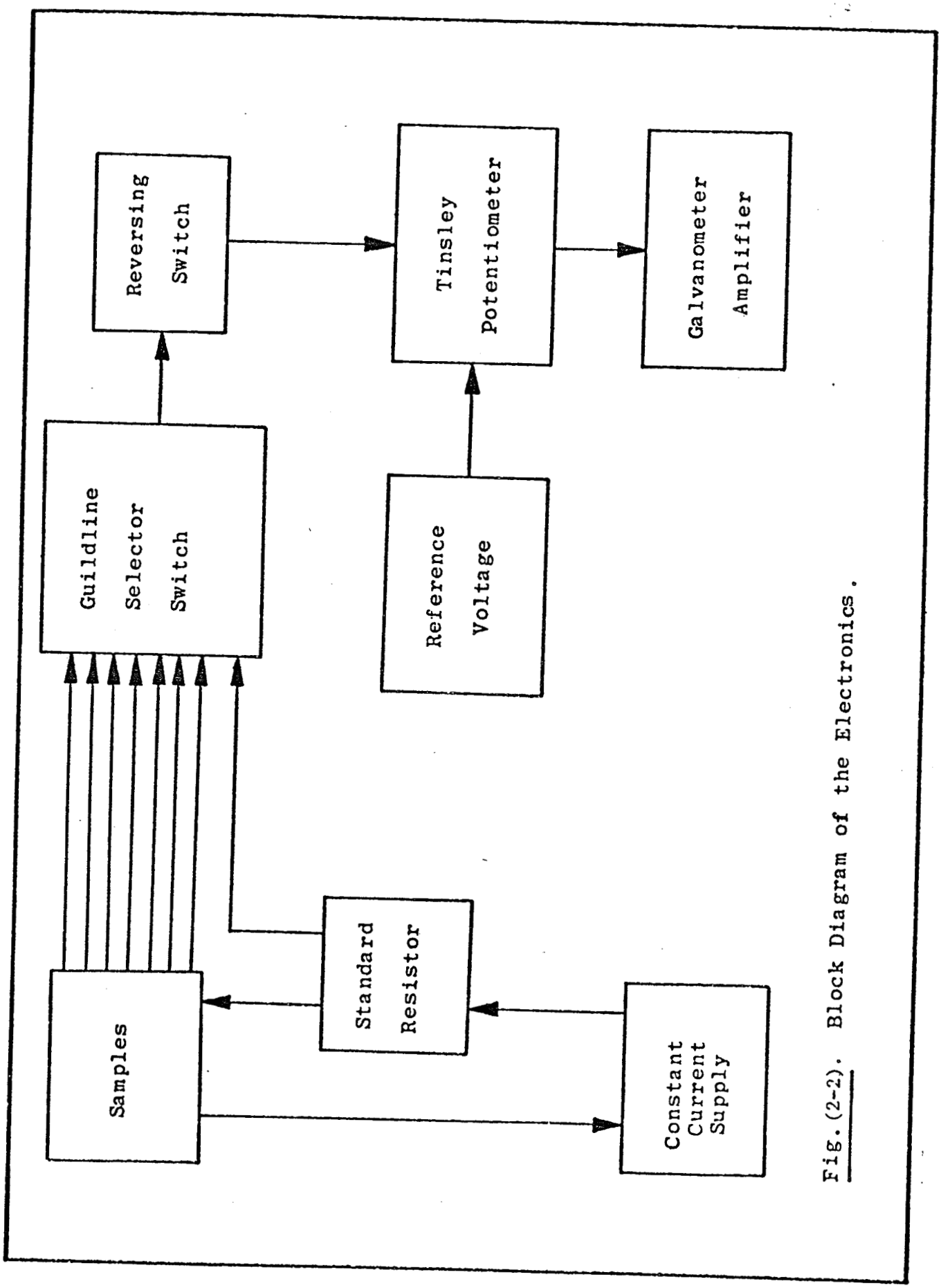

Fig. (2-2). Block Diagram of the Electronics.

standard resistor (model 9200) connected in series with the specimens, determined the current through the samples.

A Tinsley Diesselhorst thermoelectric free potentiometer (type 35 89R), in combination with a Tinsley photocell galvanometer amplifier was used to measure both the sample voltage and current, (this combination allowed reproducible potential measurements to 10^{-8} volts).

A Guildline low thermal selector switch (model 9145A10) was used to apply the voltage drop across a particular sample to the potentiometer.

The effects of thermal voltage were eliminated by using a Tinsley thermoelectric free reversing switch (type 4092) to reverse the input polarities.

The Vacuum System:

A flow diagram of the vacuum system is shown in Fig. (2-3).

A Speedivac oil diffusion pump, backed by a Speedivac (ES100) mechanical pump was used to control the pressure in the inner and outer vacuum cans.

The pressure inside the inner vacuum can (IVC) was usually about 200 microns (at 4.2K).

In order to reach the temperatures above 4.2K the pressure inside the outer vacuum can (OVC) was varied via a valve connecting it to the above pumping system. Reducing the pressure in the (OVC) reduces the heat leak from the sample block to the main He^4 both which surrounds the (OVC), and it was usual to balance this heat leak against the specimen block heater current (from the a-c Wheatston bridge) in order to produce stable temperatures above 4.2K. For temperatures above 77K, a similar procedure was followed but now using liquid N_2 in the main bath.

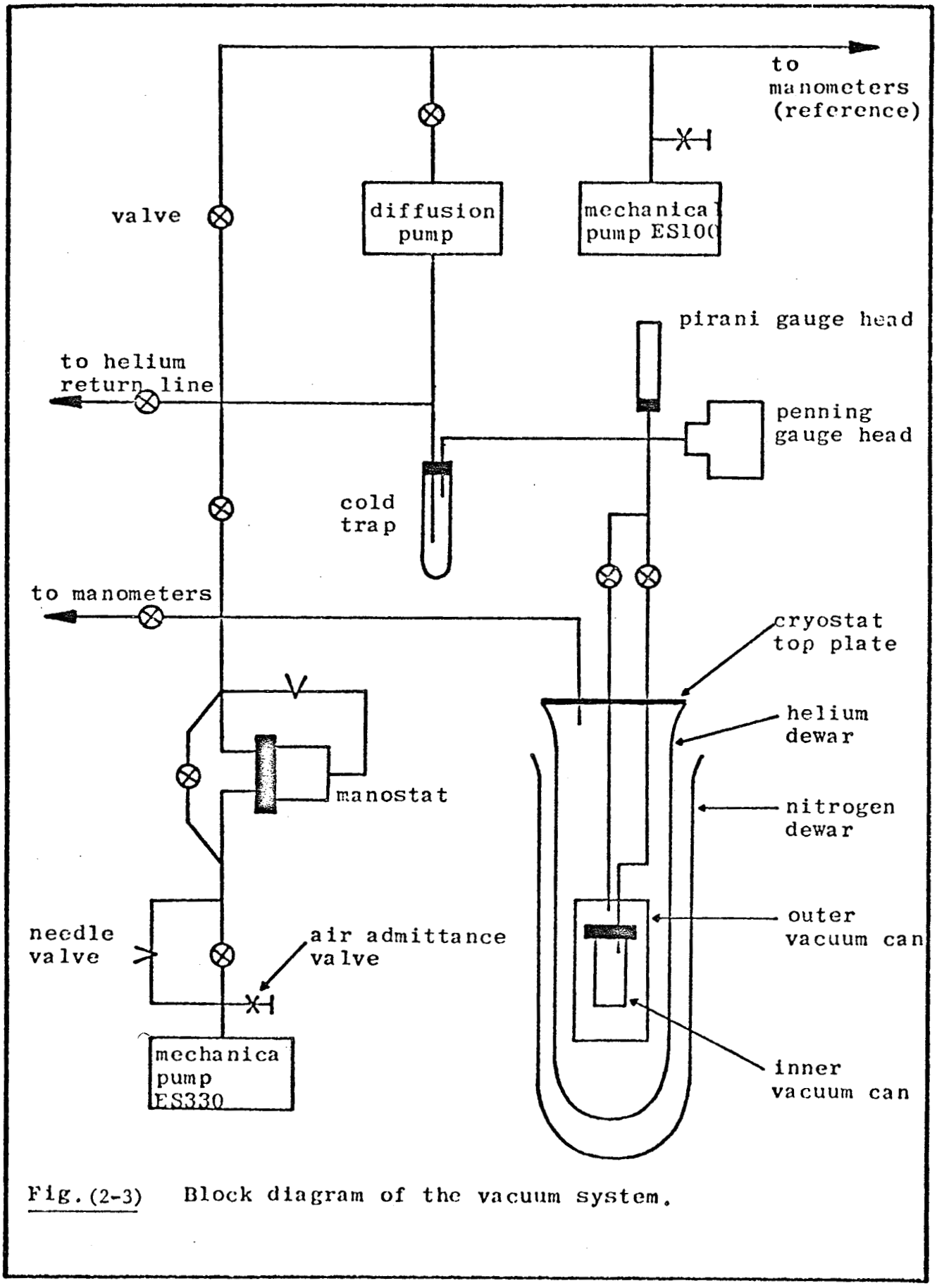

Fig. (2-3) Block diagram of the vacuum system.

The pressure monitoring system was composed of a Pirani gauge for use in the range 760 to 10^{-3} mm Hg pressure, and a Penning gauge for pressures down to 10^{-7} mm Hg.

In present study it was not necessary to achieve temperatures below 4.2K. However, these temperatures could be produced by pumping on liquid helium, using an Edwards high Vacuum Ltd. Speedivac ES 330.

A manostat device was used to achieve temperature stability in this region.

Manometers were connected to the helium bath to monitor the temperatures below 4.2K.

Sample Preparation:

The samples were prepared from 99.999% pure Pd, 99.999% Pt and 99.99% Ti (less than 10 p.p.m. from each Fe and Mn) and 99.9% V (200 p.p.m. from each silicon and Iron), all obtained from Johnson Matthey Chemicals (London, U.K.).

The most concentrated alloys, (1.0 at % Ti) in Pd and (1.0 at % Ti) in Pt and (1.0 at % V) in Pt, were prepared by melting (Pd and Ti), (Pt and Ti) and (Pt and V) in the appropriate amounts on the water-cooled copper hearth of an argon-arc furnace, using a tungsten electrode and a Ti getter.

Then Pd Ti and Pt Ti and PtV alloys containing (0.1, 0.25, 0.5, 0.75) at % Ti or V were produced by successive dilution of the most concentrated alloys.

Homogenity was ensured by inverting and remelting each alloy several times. Melting losses were negligibly small (weight losses less than 0.03%).

The button-shaped alloys, were then cold rolled to the desired

thickness between Melinex sheets (to prevent the transfer of impurities from the rollers to the alloys).

Resistivity specimens of approximate dimensions (10 Cm x 0.015 Cm x 0.3 Cm) were cut from these sheets.

Small form factors (area to length ratio) were used to yield reasonably high resistance values. Typical values for these form factors were (0.37×10^{-3} to 0.99×10^{-3} Cm). A pure metal sample also was prepared in the same manner.

To remove surface contamination, the samples were treated with a warm acid etch (containing 1/5 H_2O, 1/5 conc. HN03 and 3/5 HCl by volume plus a few drops of H_2O_2) and then washed in distilled water.

They were strain relieved by annealing at 650°C for 24 hours in a vacuum of about 10^{-5} torr.

The specimens were mounted in a holder accommodating all six samples, and their resistance measured using the previously described four-probe technique.

The absolute resistivity ρ of the samples was obtained from:

$$\rho = R \frac{A}{\ell} \qquad (2\text{-}1)$$

by measuring their form factors to within $\pm$ 0.5% using a technique described by Loram, Whall and Ford[3]. In this, the distance between the impressions of knife-edge supports on the samples can be accurately measured with a travelling microscope.

The total length of the specimen was also measured with travelling microscope.

From the density and an accurate measurement of the weight, the volume of the sample is determined.

The density is determined from lattice spacing data, using the formula:

$$\text{Density} = \frac{4}{Na^3}\,(A_1\, n_1 + A_2\, n_2) \qquad (2\text{-}2)$$

where N is Avogadro's number, A_1 and A_2 are the atomic weights of the elements used, n_1 and n_2 their fractional atomic compositions. The factor 4 enters the formula because Pd and Pt have f.c.c. structure and there are four atoms per unit cell.

The lattice spacing "a" of 1.0 at % Ti in Pd sample was measured using x-ray powder photography, and it was concluded that the change in the lattice spacing from pure Pd to the most concentrated alloy was no more than 0.01%.

In this latter measurement a cylindrical camera was used. A beam of Fe^{26} $K\alpha$ radiation ($K\alpha_1 = 1.9357A^\circ$ and $K\alpha_2 = 1.93991A^\circ$) was employed and the exposure time was four hours.

The photograph has a diffraction pattern of lines. From measurements of the position of a line, the Bragg angle, θ, of the line can be derived.

There are several effects that cause the lines to be displaced from their true positions, so that the measured angles will not be the true Bragg angles. But a small error in θ should produce a vanishingly small error in "a" as θ approaches 90°. This can be done by determining "a" from several reflections with different θ's and extrapolating the result to $\theta = 90°$.

For high angle, the following formula was used to find θ[4]:

$$\theta = 90 - 45\,\frac{S}{T} \qquad (2\text{-}3)$$

where T is half the circumference of camera and is the distance between the average of the mid-positions of the low-order and high-order, S is the separation of any pair of high-order lines.

From the value of θ for each line a value of the cell dimension "a" can be derived from the relation:

$$a = \frac{1}{2} \sqrt{N}\, \lambda \text{ cosec } \theta \qquad (2\text{-}4)$$

where $N = h^2 + k^2 + \ell^2$.

The values of "a" are then plotted against the corresponding value of $\frac{1}{2}\left(\frac{\cos^2\theta}{\theta} + \frac{\cos^2\theta}{\sin\theta}\right)$.

If there is no error due to eccentricity of the specimen the resulting points should be randomly distributed about a straight line.

The higher accuracy of the points for which θ is near 90° requires that these should be given more weight in the drawing of the line.

The point where the straight line cuts the vertical line for which $\theta = 90°$ gives the value of a, which is the value of the cell dimension at the temperature at which the photograph was taken.

The value $a = 3.89023A°$ which was found for the (1.0 at % Ti in Pd) is about 0.01% less than the value for pure Pd, 3.8907.

Having determined the length and volume (mass/density), one can then obtain the average cross sectional area, $A = \frac{V}{\ell}$.

The errors in the determination of form factor $\left(\frac{A}{\ell}\right)$, can lead to large uncertainties in $\Delta\rho$, particularly at high temperatures where $\Delta\rho$ may be a small fraction of the total resistivity.

The form factors can be determined to within $\pm$ 0.5%, even if

there is significant irregularity in the cross-sectional area of the specimen.

References

1. A.D.C. Grassie, G.A. Swallow, G. Williams and J.W. Loram, Phys. Rev., B3, 4154, (1971).

2. M.E. Colp, Transport Measurements on Some Dilute Alloys: Pd Co and Ru Mn", Thesis (U. of M.), 1972, Unpublished.

3. J.W. Loram, T.E. Whall and P.J. Ford, Phys. Rev. B2, 857, (1970).

4. N.F.M. Henry, H. Lipson and W.A. Wooster, "The interpretation of x-ray diffraction photographs", Macmillan & Co., Ltd., (1961).

CHAPTER THREE

RESULTS AND DISCUSSION

Introduction

Up to the present time, there has not been a detailed study of the two-band model in dilute Pt and Pd based alloys.

To summarize the work that has been done, DMR were observed by De Haas and De Boer[1] in measuring the resistivity of pure platinum. They found DMR due to physical impurities (mechanical deformation) at temperatures above 10°K.

Krautz and Schultz[2] suggested using the K.S.W. equation

$$\frac{1}{\Delta(T)} = \frac{1}{\gamma\rho_p} + \frac{1}{\beta\rho_o} \qquad (3\text{-}1)$$

with constant coefficients γ and β to correct for DMR, while Klemens and Lowenthal[3] in an analysis of the resistivity-temperature relationship of 17 platinum resistors as determined in various laboratories show that DMR can be classed in different groups, in one of them, the two-band model works satisfactorily but combination of data from different laboratories gives a complex form for DMR which is not consistent with K.S.W. equation even when γ and β vary with temperature.

The only quantitative study of DMR in Pt alloys of known impurity content was made by Stewart and Huebener[4], who measured the electrical resistance of pure Pt, four dilute Pt Au alloys and one concentrated Pt Rh alloy from 4.2 to 300K. They used the two-band model with constant γ and β to calculate DMR at all temperatures. However, in order to explain the low temperature maximum which appeared in the low concentration Pt Au alloys (about 30-50K), they found it necessary to make γ and β temperature-dependent.

In the case of Pd, there is no clear example of deviation from Matthiessen's Rule in dilute Pd based alloys which do not manifest

resistivity minimum.

In the present work, the temperature dependence of the resistivity of dilute Pd and Pt based alloys was investigated over a temperature range from 4.2 to 300K.

The experimental results can be explained on the basis of the two band model with constant β and temperature-dependent γ in Pt Ti and PtV alloys and temperature-dependent β and γ in the case of Pd Ti alloys.

Results and Discussion

The resistivities of samples were calculated using the experimentally determined electrical resistance of the samples as a function of temperature and their geometrical form factor.

Small errors in the determination of the gometrical form factor can lead to serious errors in the determination of $\Delta(T)$ from resistance values, particularly at high temperatures where total resistivity is large.

In the case of $\rho_{solvent} >> \Delta(T)$, the errors can be very large.

Alley and Serin[5] and other workers[3] have normalized the resistance data by dividing by the ice point values, which cancels the geometrical factor assuming thermal expansion effects to be negligible.

In order to compare the experimental results with the predictions of Matthiessen's Rule, we define $\Delta(T)$ by the relation:

$$\Delta(T) = \rho_{tot} - (\rho_{ph} + \rho_o) \qquad (3\text{-}2)$$

where ρ_o is the resistivity of the specimen as measured at 4.2K.

As can be seen in Figures (3-1) to (3-5), the temperature

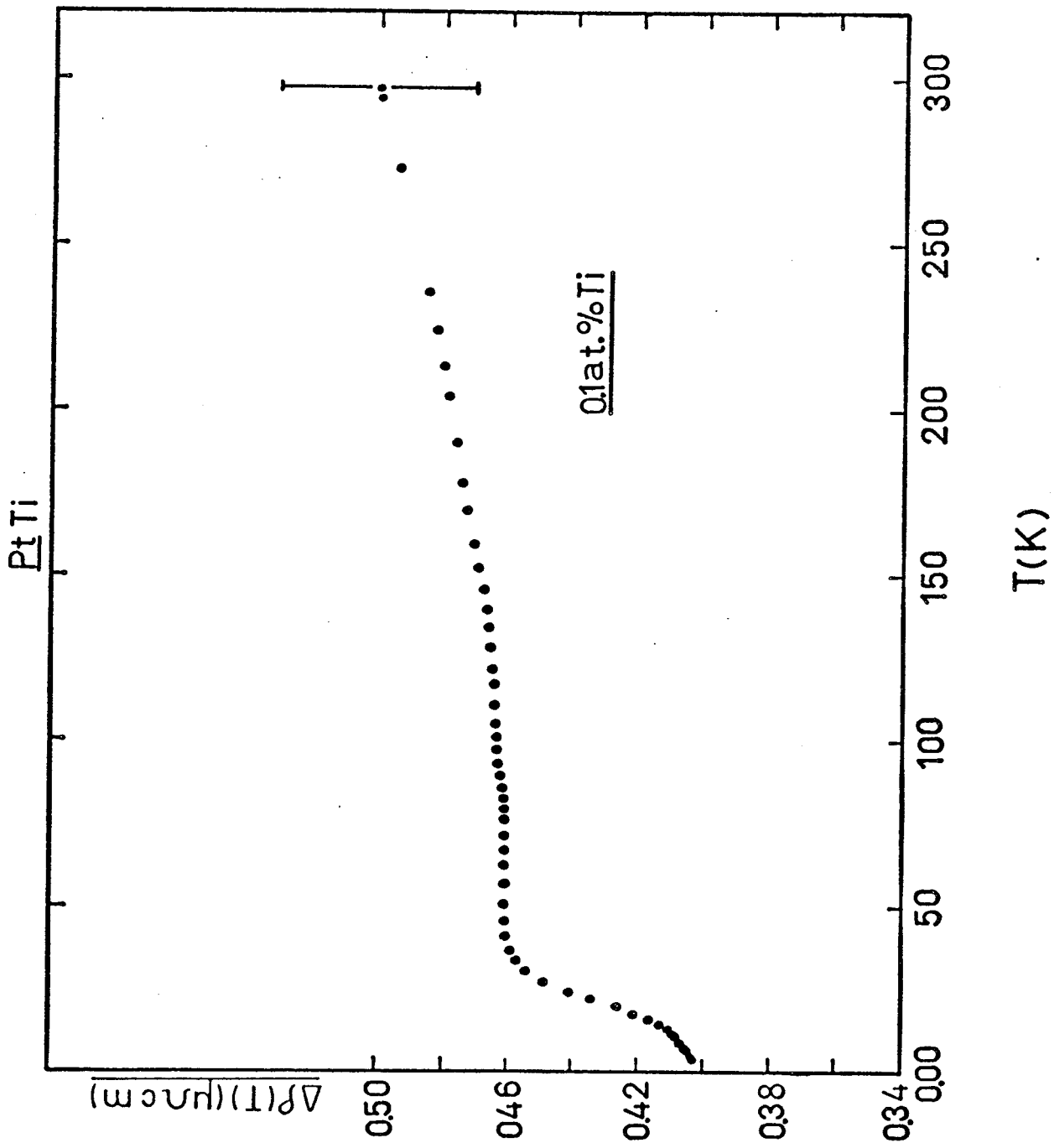
Pt Ti
0.1at.%Ti
Δρ(T)(μΩcm)
0,50
0,46
0,42
0,38
0,34
0,00
50
100
150
200
250
300
T(K)

Fig. (3-1)

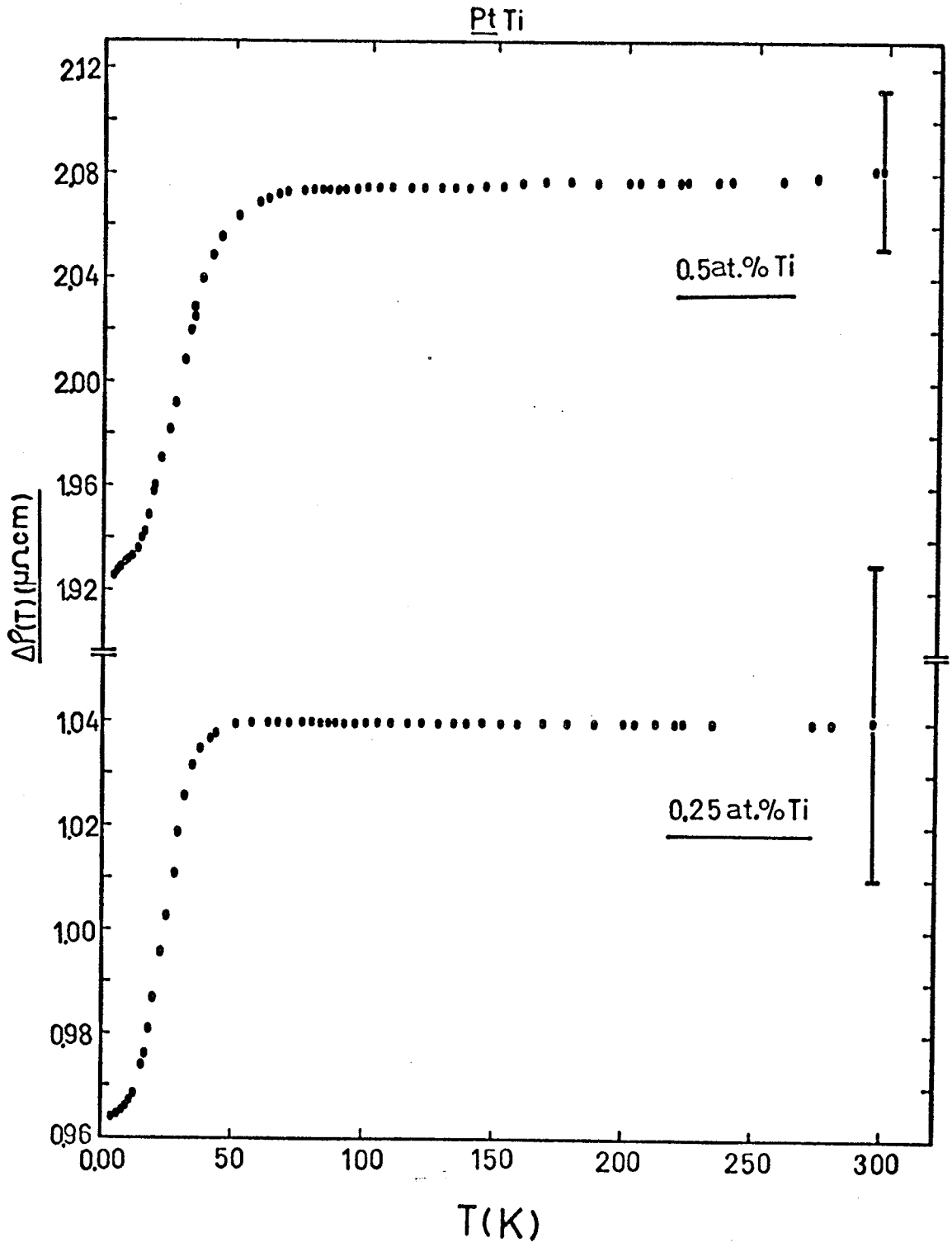
Pt Ti
2.12
2.08
2.04
2.00
1.96
1.92
1.04
1.02
1.00
0.98
0.96
0.00
50
100
150
200
250
300
Δρ(T) (μΩcm)
T(K)
0.5at.% Ti
0.25 at.% Ti

Fig. (3-2)

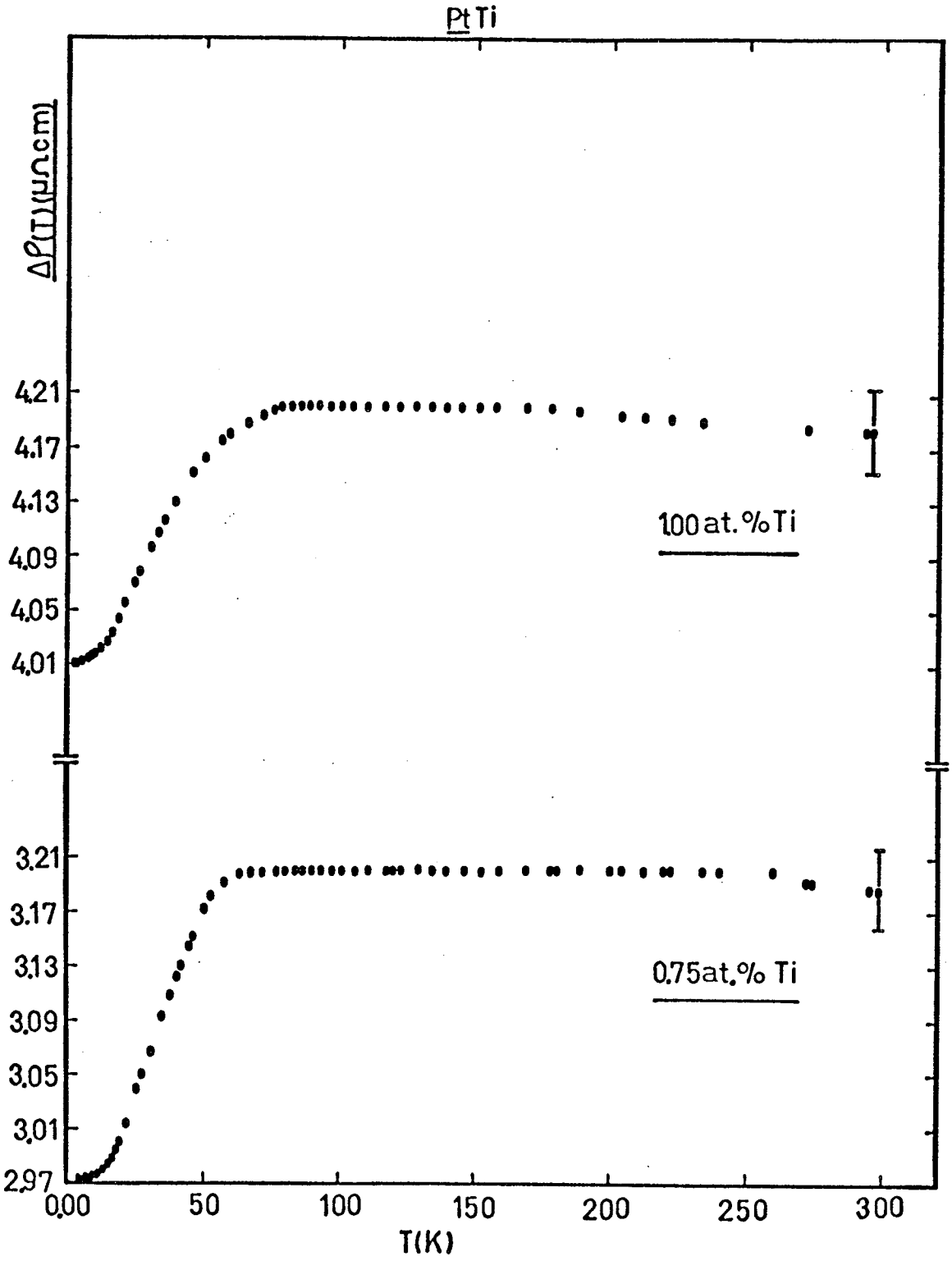
Pt Ti
Δρ(T)(μΩcm)
4.21
4.17
4.13
4.09
4.05
4.01
1.00 at.% Ti
3.21
3.17
3.13
3.09
3.05
3.01
2.97
0.75at.% Ti
0.00
50
100
150
200
250
300
T(K)

Fig. (3-3)

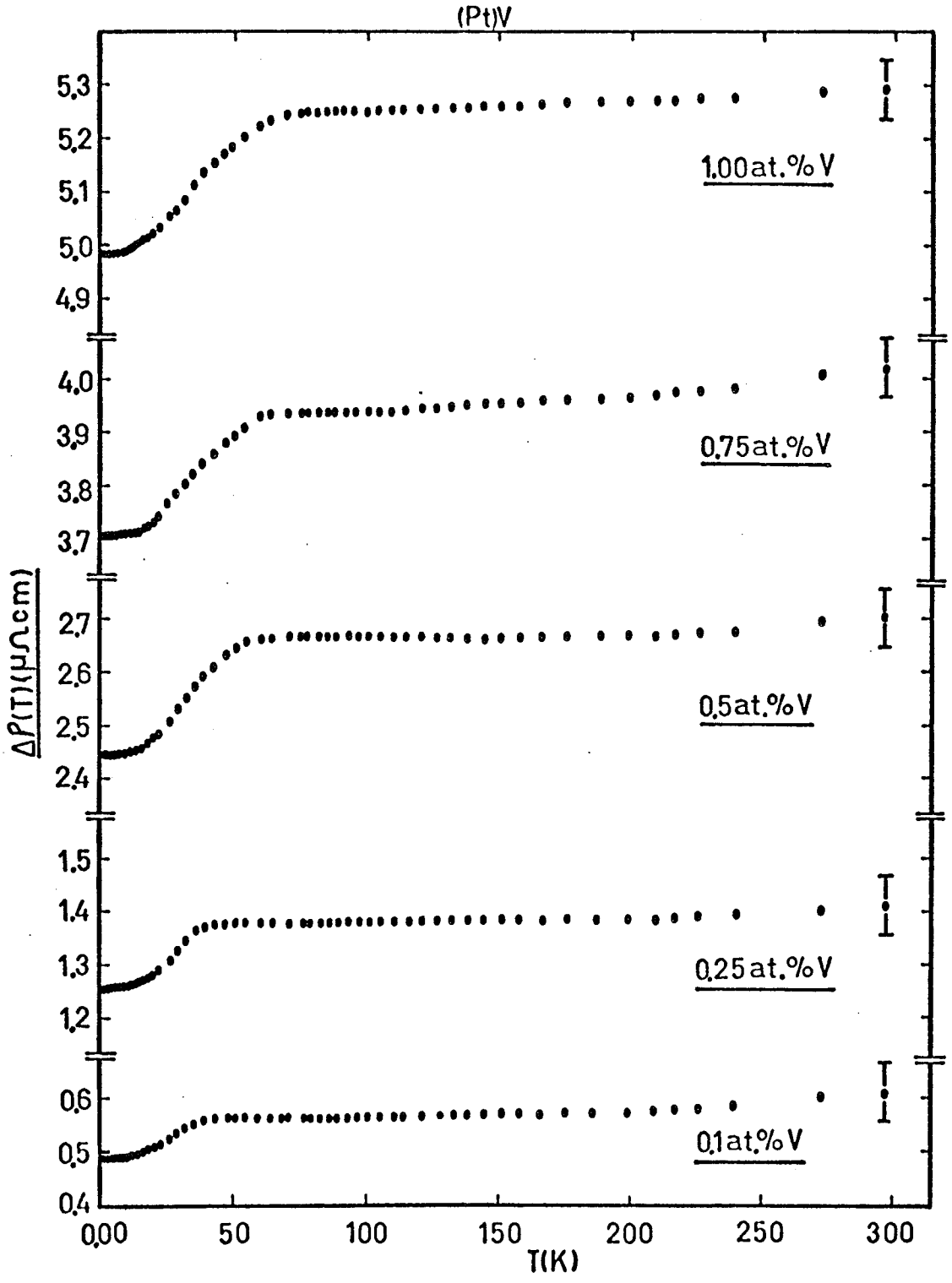
(Pt)V
1.00at.%V
0.75at.%V
0.5at.%V
0.25at.%V
0.1at.%V
ΔP(T)(μΩcm)
T(K)
5.3
5.2
5.1
5.0
4.9
4.0
3.9
3.8
3.7
2.7
2.6
2.5
2.4
1.5
1.4
1.3
1.2
0.6
0.5
0.4
0.00
50
100
150
200
250
300

Fig. (3-4)

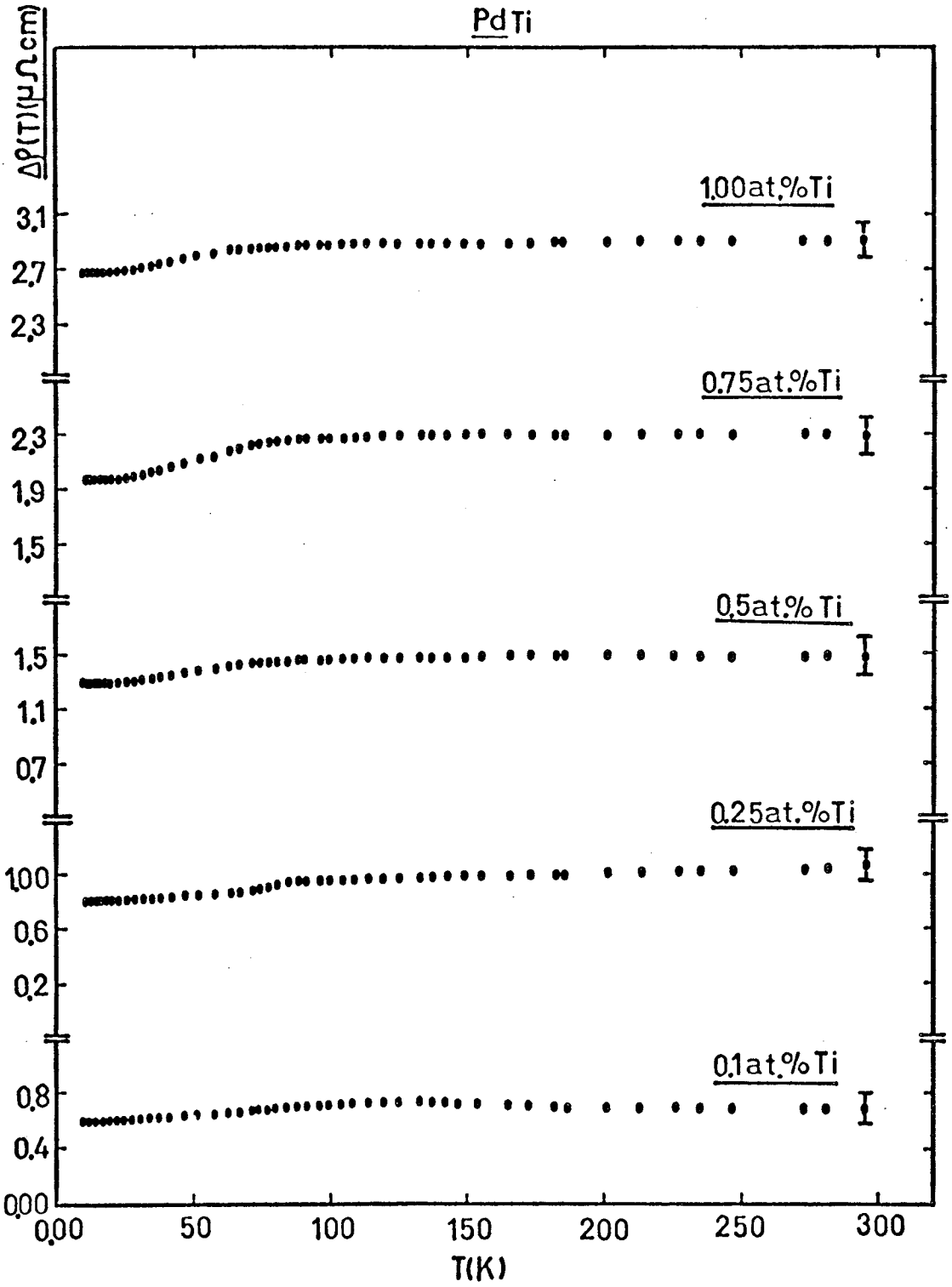
PdTi
Δρ(T)(μΩcm)
1.00at.%Ti
0.75at.%Ti
0.5at.%Ti
0.25at.%Ti
0.1at.%Ti
3.1
2.7
2.3
2.3
1.9
1.5
1.5
1.1
0.7
1.00
0.6
0.2
0.8
0.4
0.00
0.00
50
100
150
200
250
300
T(K)

Fig. (3-5)

dependence of the DMR in Pd and Pt based alloys follows approximately the form suggested by the Kohler-Sondheimer-Wilson type equation, Viz. having a sharp rise with increasing temperature at low temperatures and a temperature independent behaviour at high temperatures.

The errors in geometrical form factors are shown and the nominal concentrations are also indicated in these figures.

The Pure Pt resistivity

The pure platinum sample used in this investigation has a resistivity ratio of 2000 and a room temperature resistivity of $\rho(296K) = 10.644\ \mu\Omega$ cm.

The plot of ρ for Pt versus temperature is shown in Fig. (3-6).

At temperatures below 15K, the resistivity is well described by the expression:

$$\rho_{phonon} = \rho_o + AT^2 + BT^5 \qquad (3.3)$$

where the solid line in figure (3-7) uses:

$$A = 1.6 \times 10^{-5}\ \mu\Omega\ \text{Cm}\ K^{-2}$$

and

$$B = 1.4 \times 10^{-8}\ \mu\Omega\ \text{Cm}\ K^{-5}$$

The values are in fair agreement with the values:

$$A = 1.4 \times 10^{-5}\ \mu\Omega\ \text{Cm}\ K^{-2} \quad \text{and} \quad B = 1.1 \times 10^{-8}\ \mu\Omega\ \text{Cm}\ K^{-5}$$

found by White and Woods[6],

Analysis of the Results

The two-band model is used in an analysis of the temperature

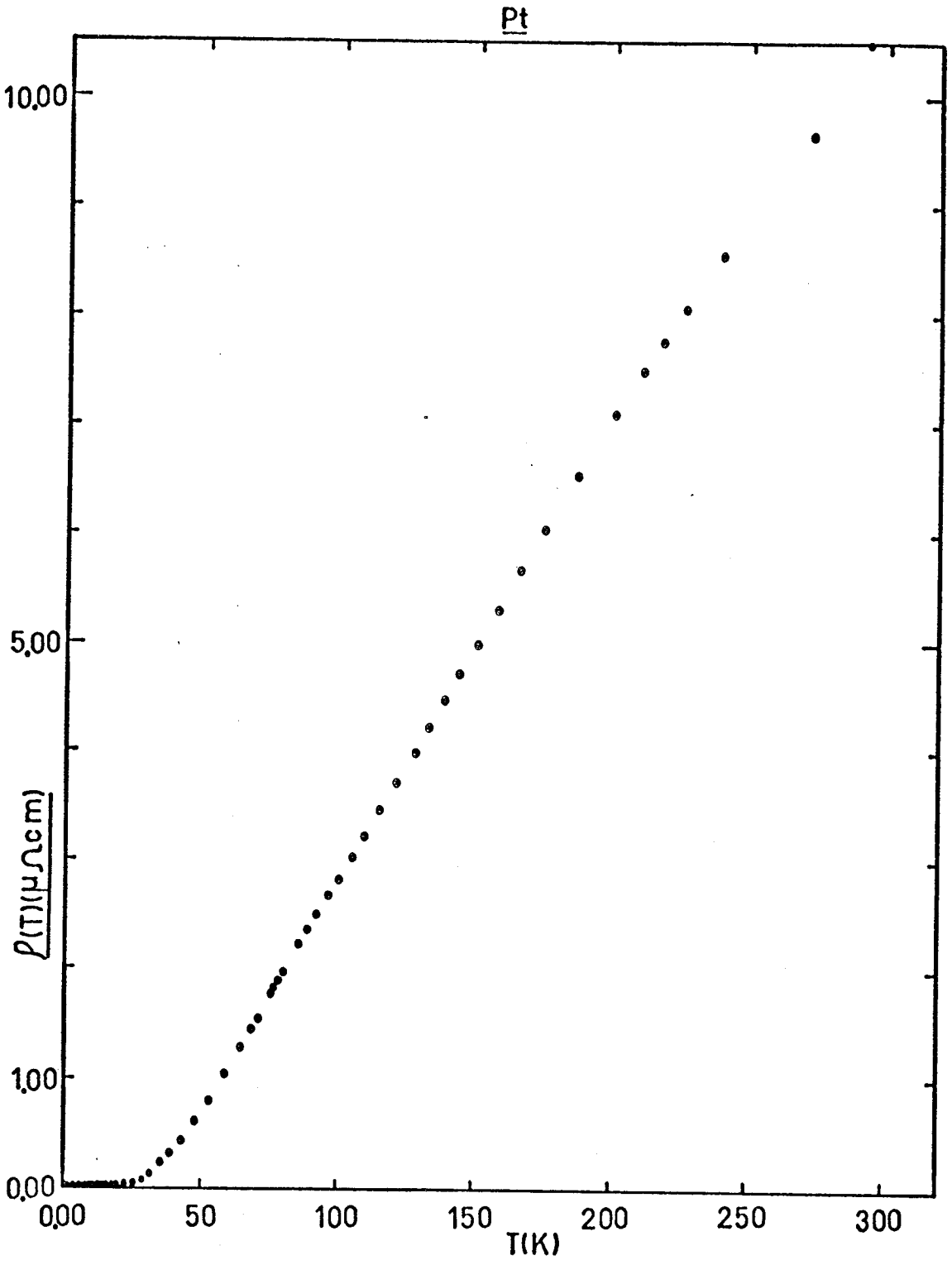

Fig. (3-6)

dependence of deviation from Matthiessen's Rule in the following manner.

By combining the equations:

$$\rho_a(C,T) = \rho_P(T) + \rho_{ia}(C,T) + \Delta(C,T) \tag{3-4}$$

and

$$\frac{1}{\Delta(C,T)} = \frac{1}{\gamma\rho_P} + \frac{1}{\beta\rho_{ia}} \tag{3-5}$$

we get:

$$\rho_a - \rho_{ia} = \rho_P + \frac{\gamma\beta\ \rho_P(T)\ \rho_{ia}(T)}{\gamma\rho_P(T) + \beta\rho_{ia}(T)} \tag{3-6}$$

In this formula, if the impurity resistivity is temperature independent we can replace ρ_{ia} in the second term by ρ_o and ρ_o is the value of $\rho_{ia}(T)$ at $T = 4.2K$.

From a plot of $\rho_a(T) - \rho_{ia}(T)$ against ρ_o at fixed temperatures we obtain:

$$\rho_a - \rho_{ia} \to \rho_P \quad \text{as} \quad \rho_o \to o \tag{3-7}$$

$$\rho_a - \rho_{ia} = \rho_P + \beta\rho_o \quad \text{if} \quad \rho_o\beta << \gamma\ \rho_P \tag{3-8}$$

$$\rho_a - \rho_{ia} = (1+\gamma)\rho_P \quad \text{if} \quad \rho_o\beta >> \gamma\ \rho_P \tag{3-9}$$

ρ_P can be determined if the intercept is clearly defined. β and γ can be determined from slope of the linear part of the graph and the constant value of $\rho_i - \rho_{ia}$ at large ρ_o (saturation region), respectively. But because the linear and saturation regions are not clearly defined at all temperatures, another procedure has been used to determine γ and β.

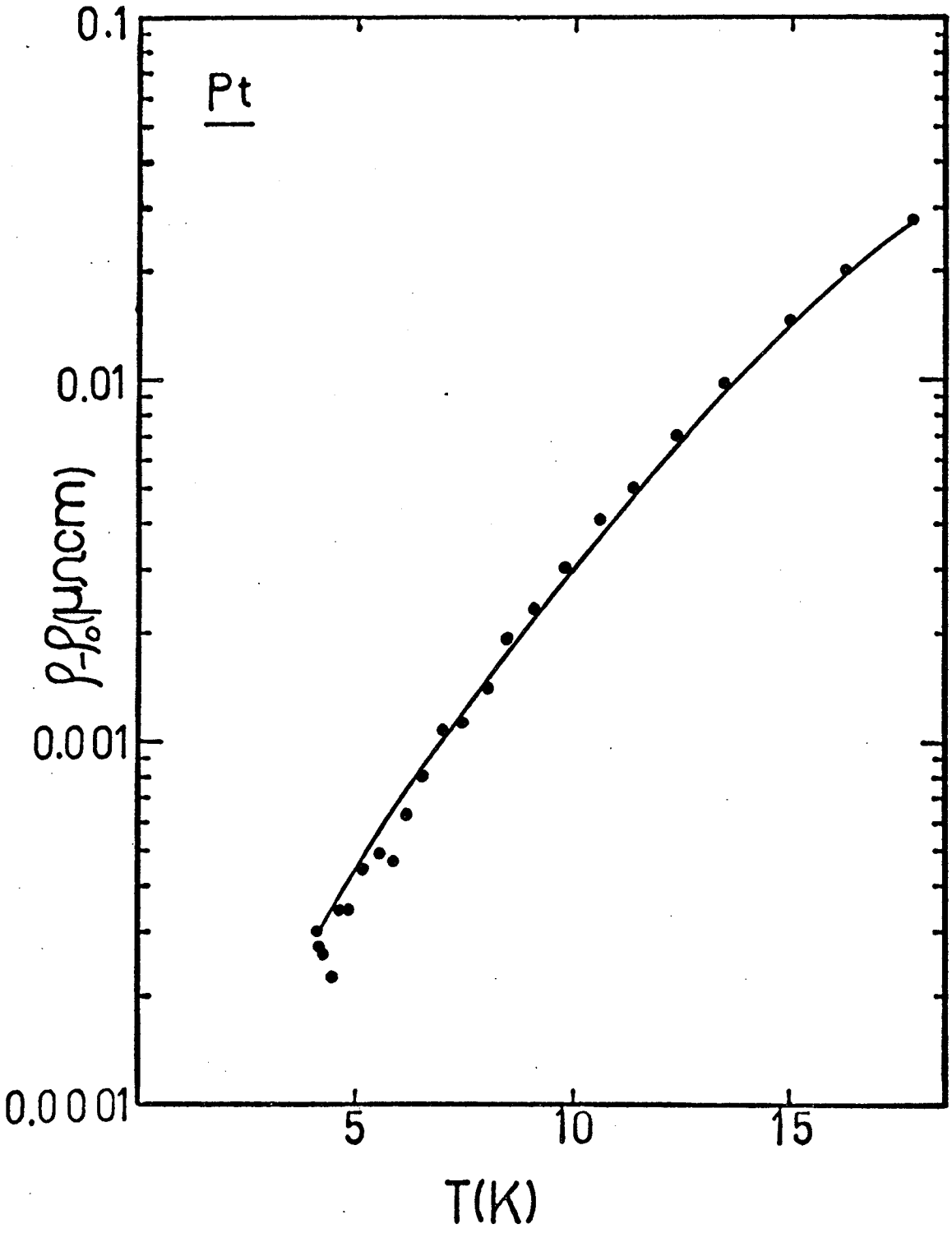

Fig. (3-7)

$\frac{1}{\Delta - \rho_o}$ is plotted against $\frac{1}{\rho_o}$ where:

$$\Delta - \rho_o = \rho_a - \rho_{ia} - \rho_P$$

A linear relation is predicted by the previous equations.

In these graphs the slope is equal to $\frac{1}{\beta}$ and the intercept is equal to $\frac{1}{\gamma\rho_P}$.

Knowing ρ_P, we can determine γ for each temperature. ρ_P is equal to ρ_{metal} (which can be found from the graph of ρ_{metal} versus temperature) after substracting $\rho_o + \rho_{para}$ from it.

Plots of $\frac{1}{\Delta - \rho_o}$ versus $\frac{1}{\rho_o}$ at different fixed temperatures for Pt Ti alloys are shown in figures (3-8), (3-9) and (3-10).

Values of β and γ have been determined at a series of temperatures.

In Pt Ti alloys β is independent of temperature and equal to 0.24, although γ is temperature-dependent.

Plots of γ versus temperature for different concentrations are shown in Figure (3-11).

Plots of $\frac{1}{\Delta - \rho_o}$ against $\frac{1}{\rho_o}$ at different fixed temperatures for Pt V are shown in Figures (3-12), (3-13) and (3-14).

For these alloys β is independent of temperature and equal to 0.22, while γ is dependent on temperature and the plots of γ versus temperature for different concentrations are shown in Figure (3-15).

In the case of Pd Ti alloys we could not fit the experimental values by using a temperature independent β, so we allowed both β and γ to vary with temperature.

Plots of $\frac{1}{\Delta - \rho_o}$ against $\frac{1}{\rho_o}$ for these alloys are shown in

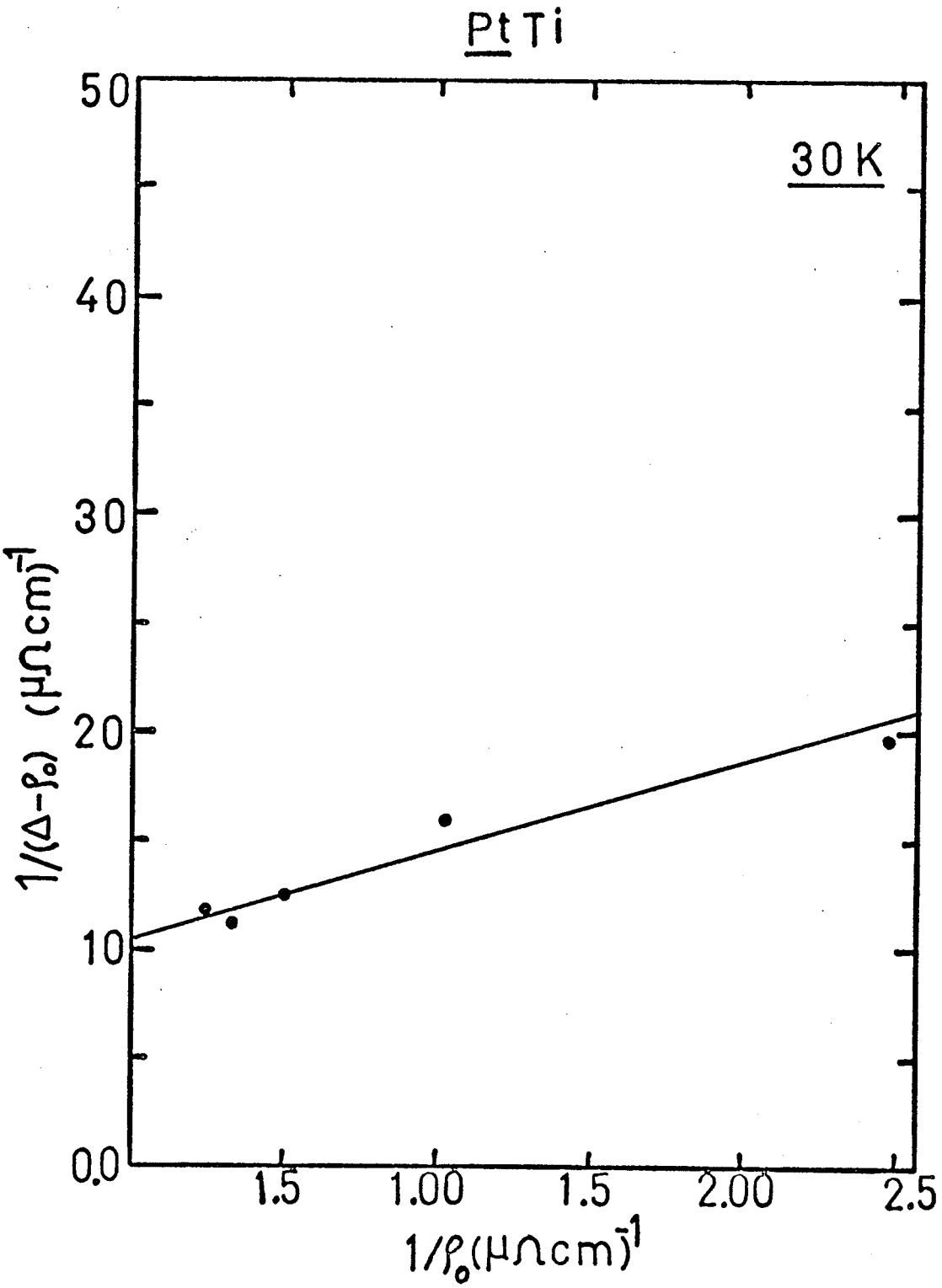

Fig. (3-8)

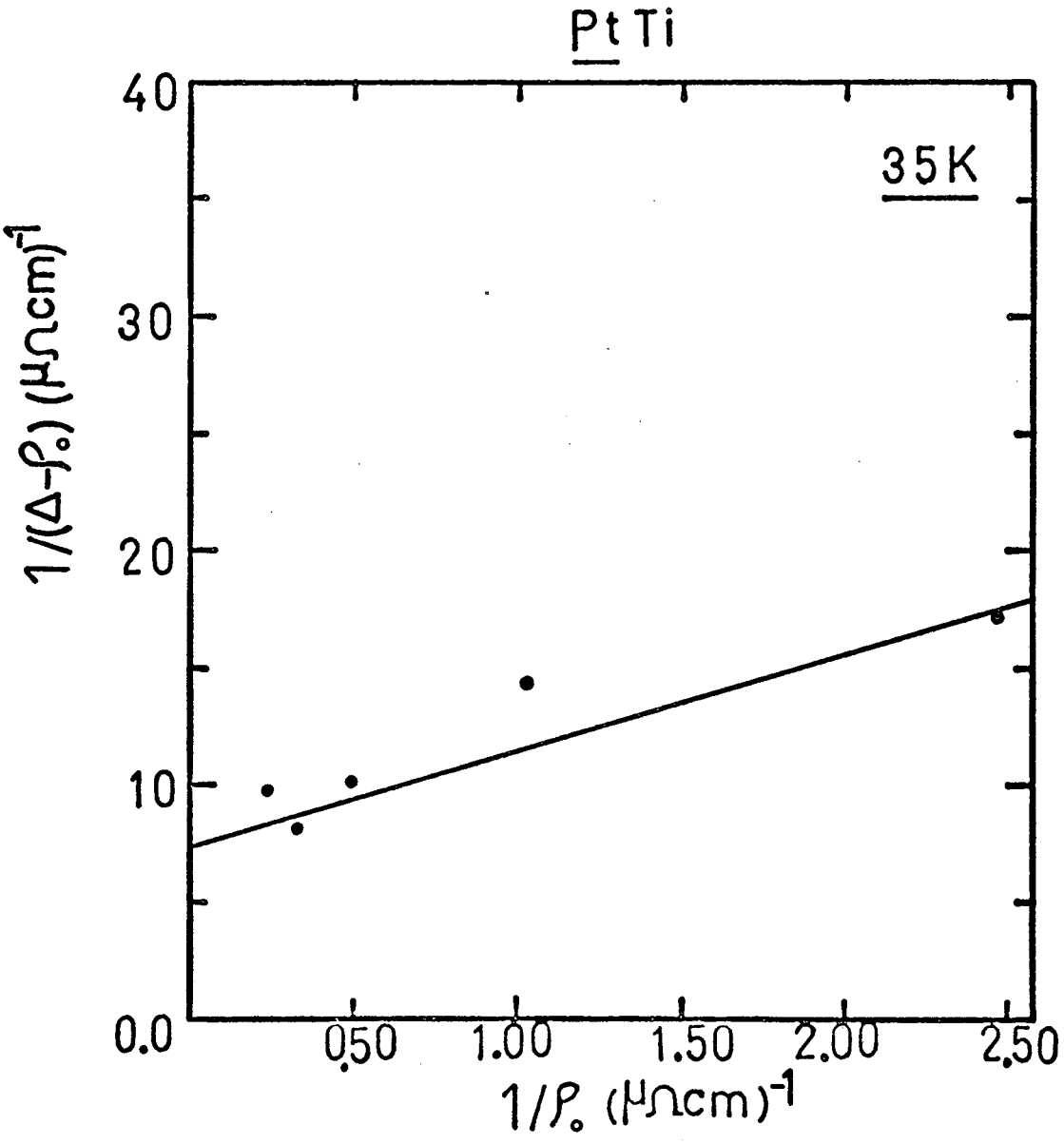

Fig. (3-9)

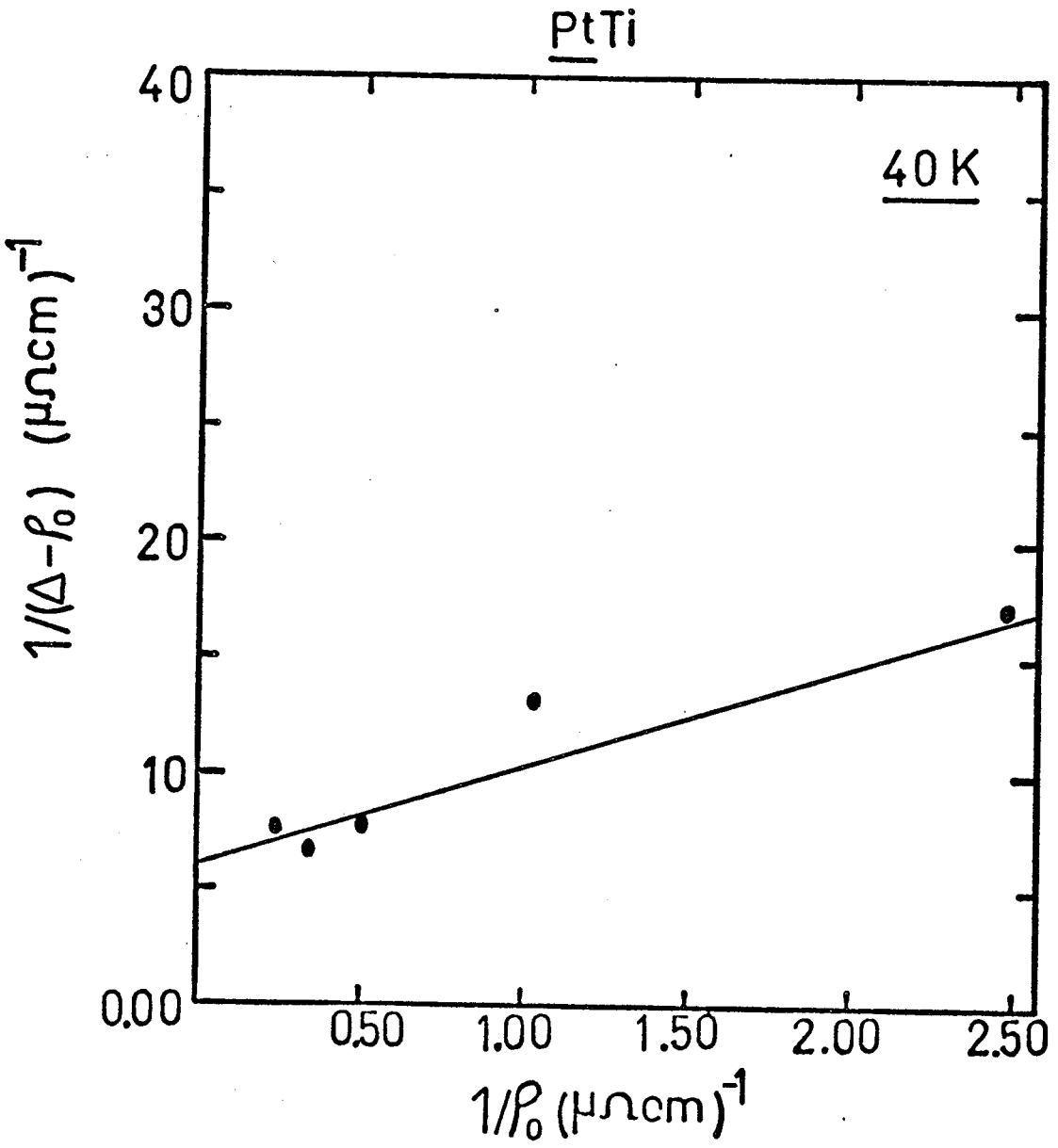
PtTi
40 K
40
30
20
10
0.00
0.50
1.00
1.50
2.00
2.50
$1/(\Delta-\rho_0)$ $(\mu\Omega cm)^{-1}$
$1/\rho_0$ $(\mu\Omega cm)^{-1}$

Fig. (3-10)

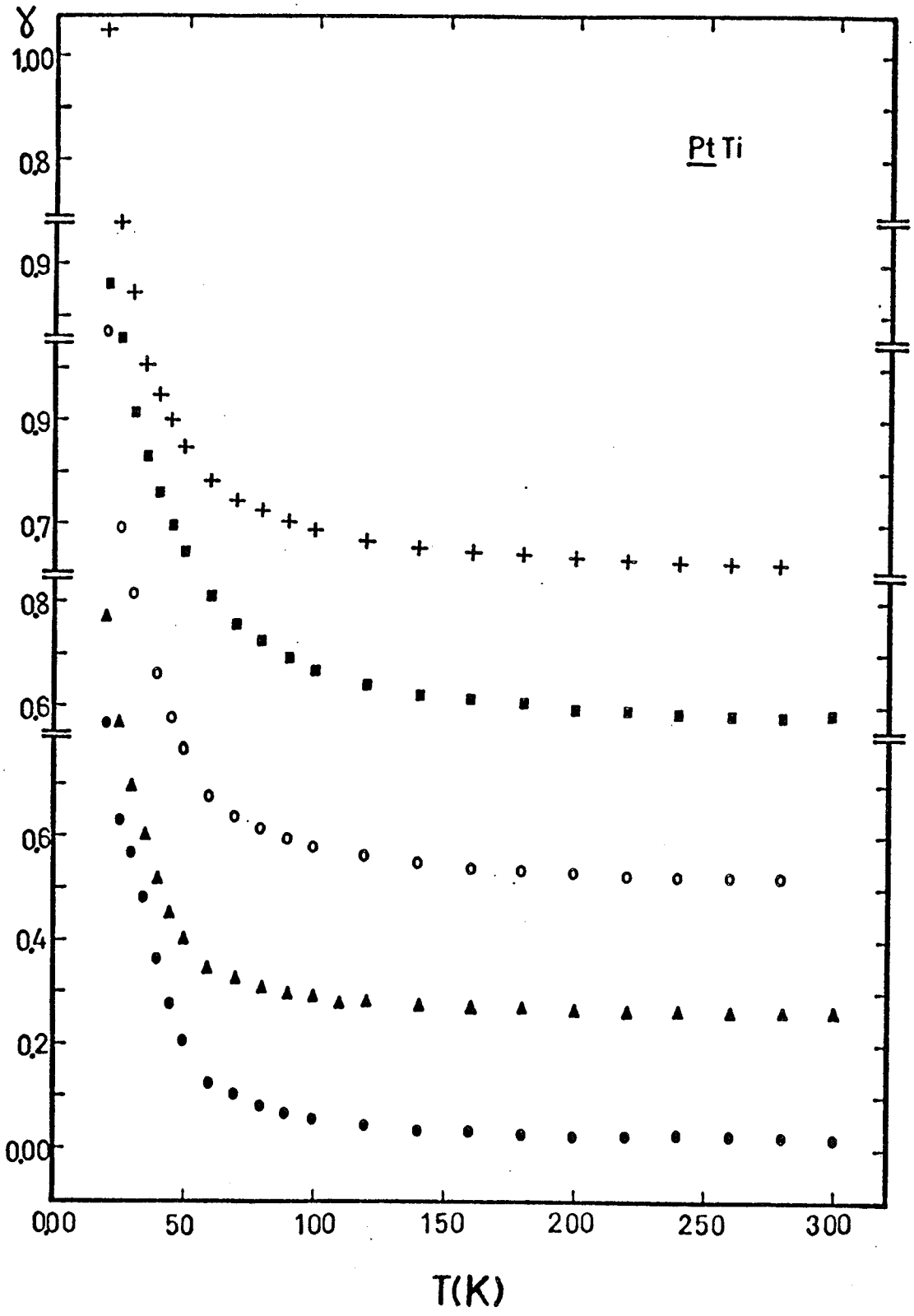
χ
1.00
0.8
0.9
0.9
0.7
0.8
0.6
0.6
0.4
0.2
0.00
Pt Ti
0.00
50
100
150
200
250
300
T(K)

Fig. (3-11)

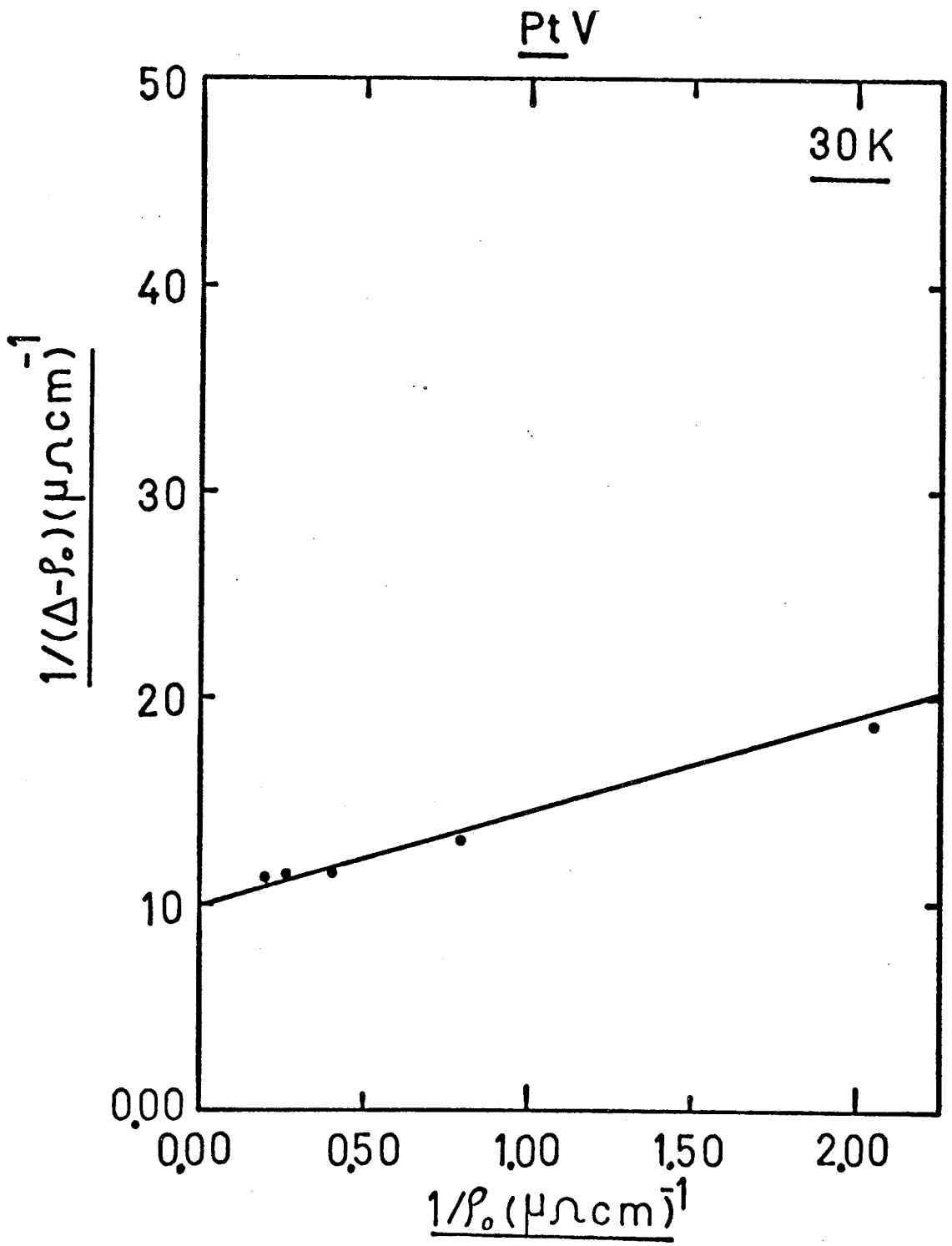
Pt V
30 K
50
40
30
20
10
0.00
0.00
0.50
1.00
1.50
2.00
1/(Δ-ρ₀)(μΩcm)⁻¹
1/ρ₀(μΩcm)⁻¹

Fig. (3-12)

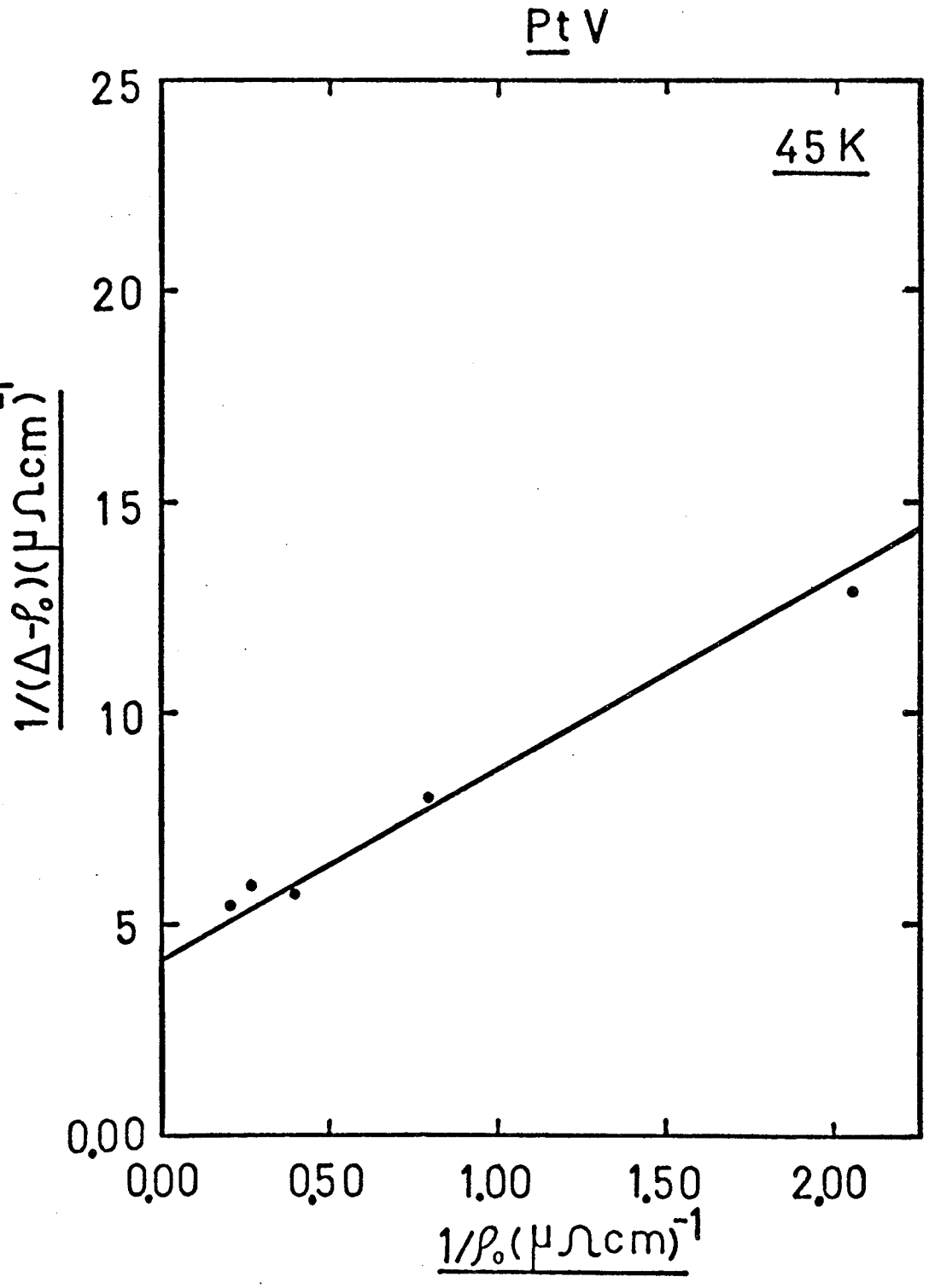
Pt V
45 K
25
20
15
10
5
0.00
0.00
0.50
1.00
1.50
2.00
1/(Δ-ρ₀)(μΩcm)⁻¹
1/ρ₀(μΩcm)⁻¹

Fig. (3-13)

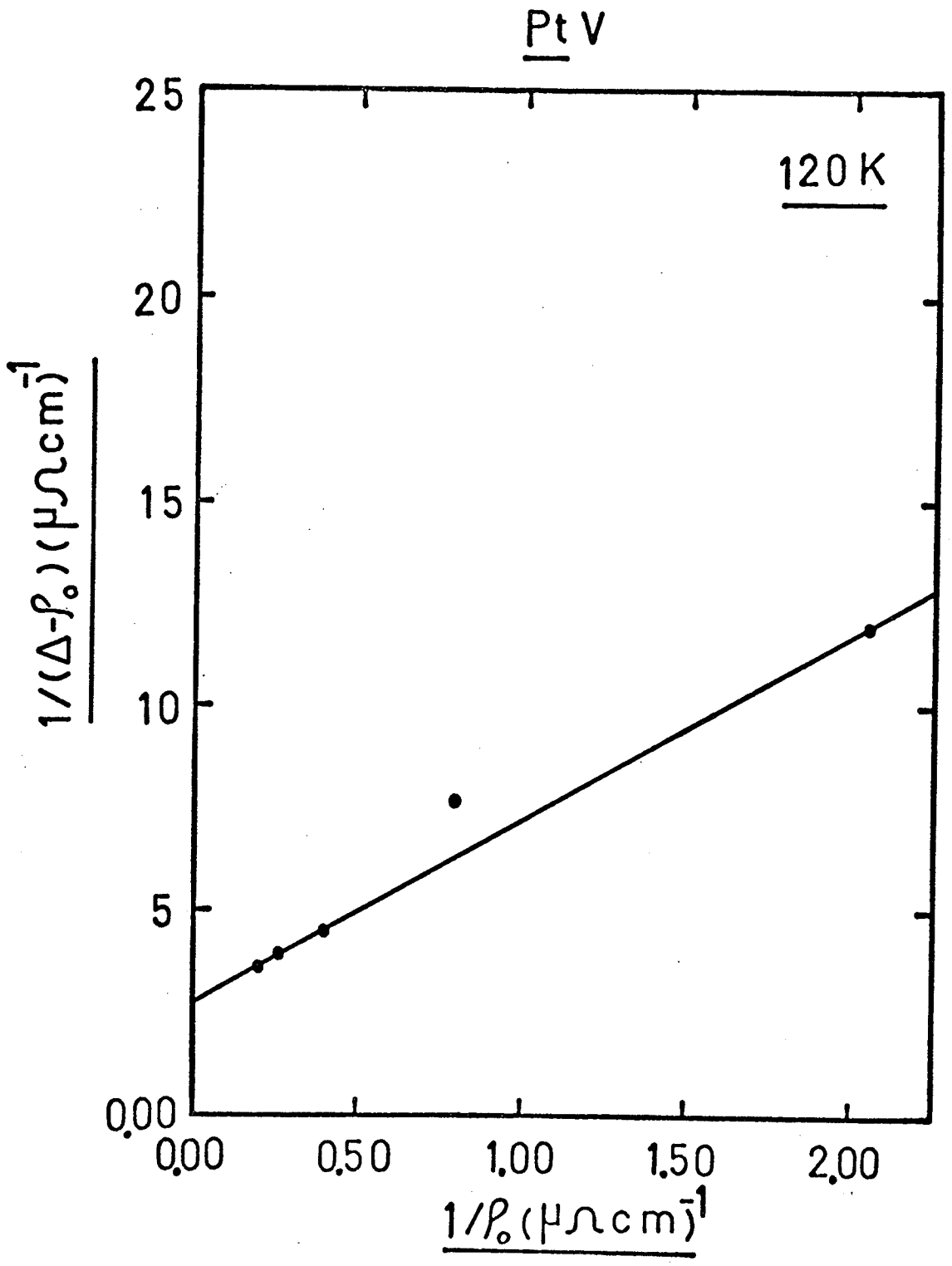
Pt V
120 K
25
20
15
10
5
0.00
0.00
0.50
1.00
1.50
2.00
1/(Δ-ρ₀) (μΩcm)⁻¹
1/ρ₀ (μΩcm)⁻¹

Fig. (3-14)

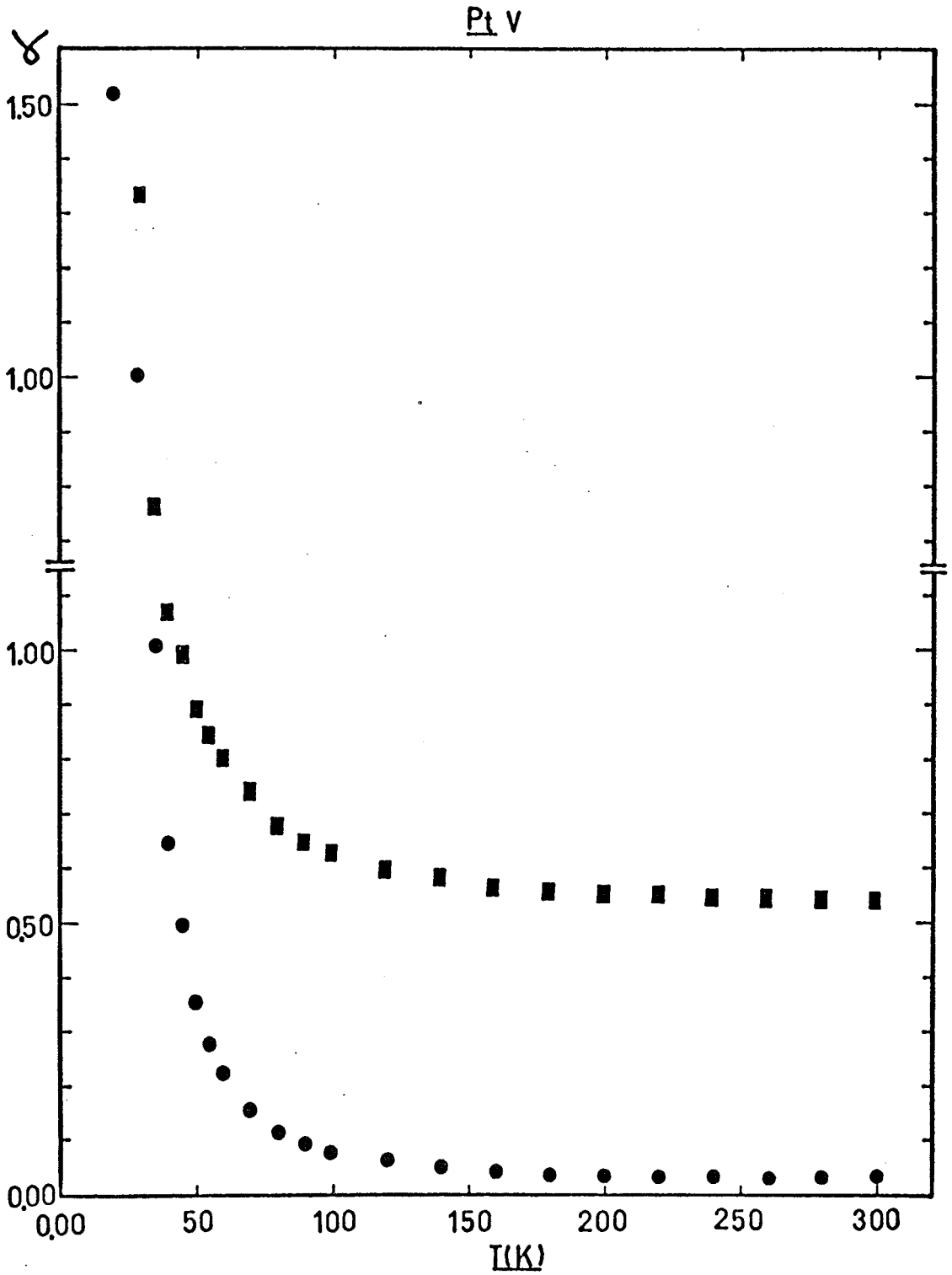

Fig. (3-15)

Figures (3-16), (3-17) and (3-18).

The values of β for each temperature are shown in Table (3-1).

The graphs of γ versus temperature for different concentrations are shown in Figure (3-19).

In Pd Ti alloys deviations below 40K were small and we did not get a smooth variation for γ below 40K but above this temperature we get a smooth variation of γ with temperature.

Knowing the values of β and γ, the parameters α_i and α_p have been calculated.

α_i is the ratio of the conductivity σ_N (on the neck) to that on the belly (σ_B) of the Fermi surface when the scattering is due to impurity and α_p is the same ratio when the scattering is due to phonon alone.

These values can be found from the formula:

$$\gamma = \frac{1}{\alpha_p} \left(\frac{\alpha_i - \alpha_p}{1 + \alpha_i}\right)^2 \qquad (3\text{-}10)$$

and

$$\beta = \frac{1}{\alpha_i} \left(\frac{\alpha_i - \alpha_p}{1 + \alpha_p}\right)^2 \qquad (3\text{-}11)$$

(Appendix 1)

By inverting these equations we get[4]:

$$\alpha_i = 1 + \frac{1}{2} a \pm \frac{1}{2} a \left(1 + \frac{4}{a}\right)^{\frac{1}{2}} \qquad (3\text{-}12)$$

$$\alpha_p = 1 + \frac{1}{2} b \pm \frac{1}{2} b \left(1 + \frac{4}{b}\right)^{\frac{1}{2}} \qquad (3\text{-}13)$$

where a and b are defined by:

$$a \equiv (\gamma - \beta - \beta\gamma)^2 / \beta\gamma^2 \qquad (3\text{-}14)$$

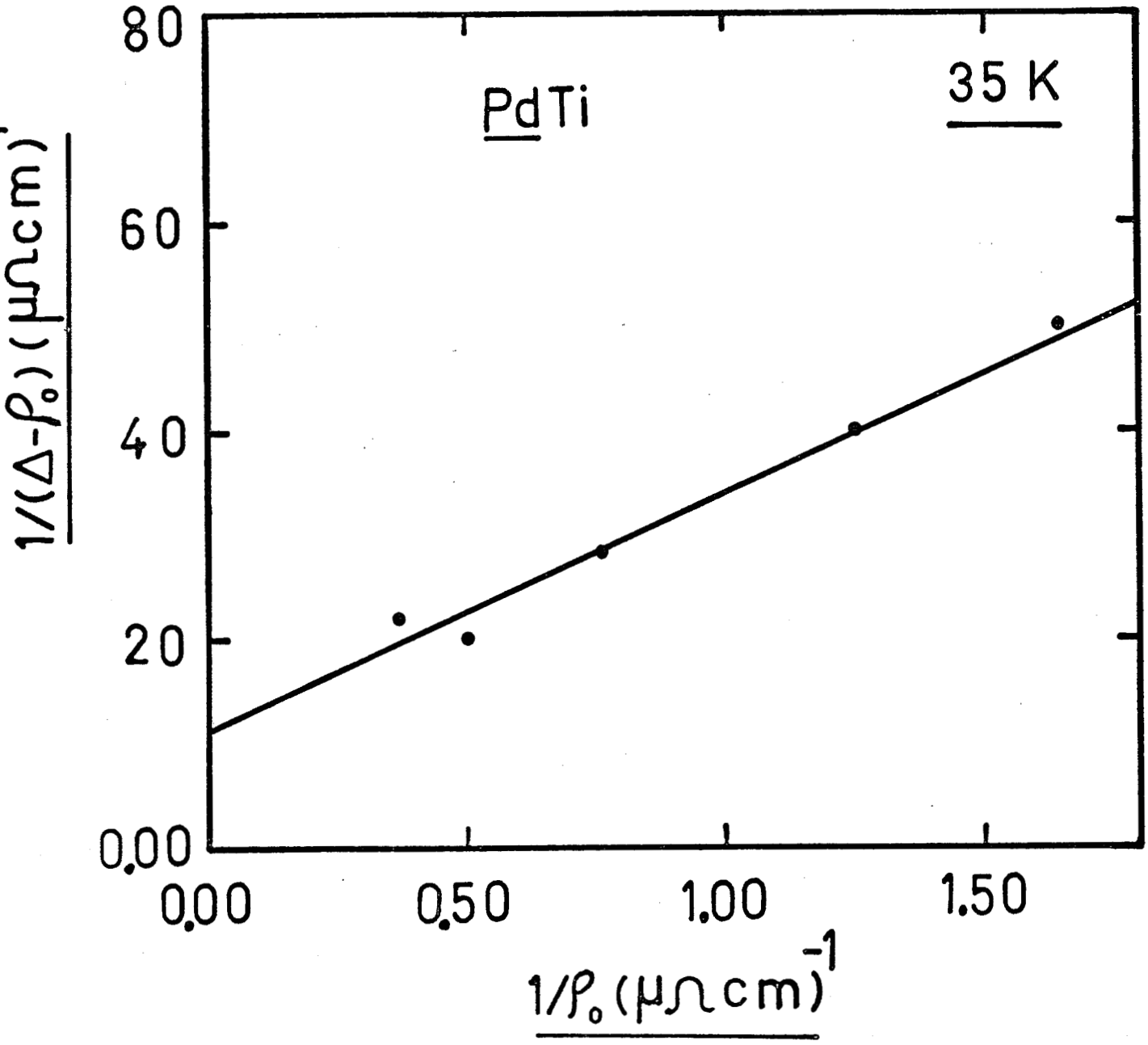

Fig. (3-16)

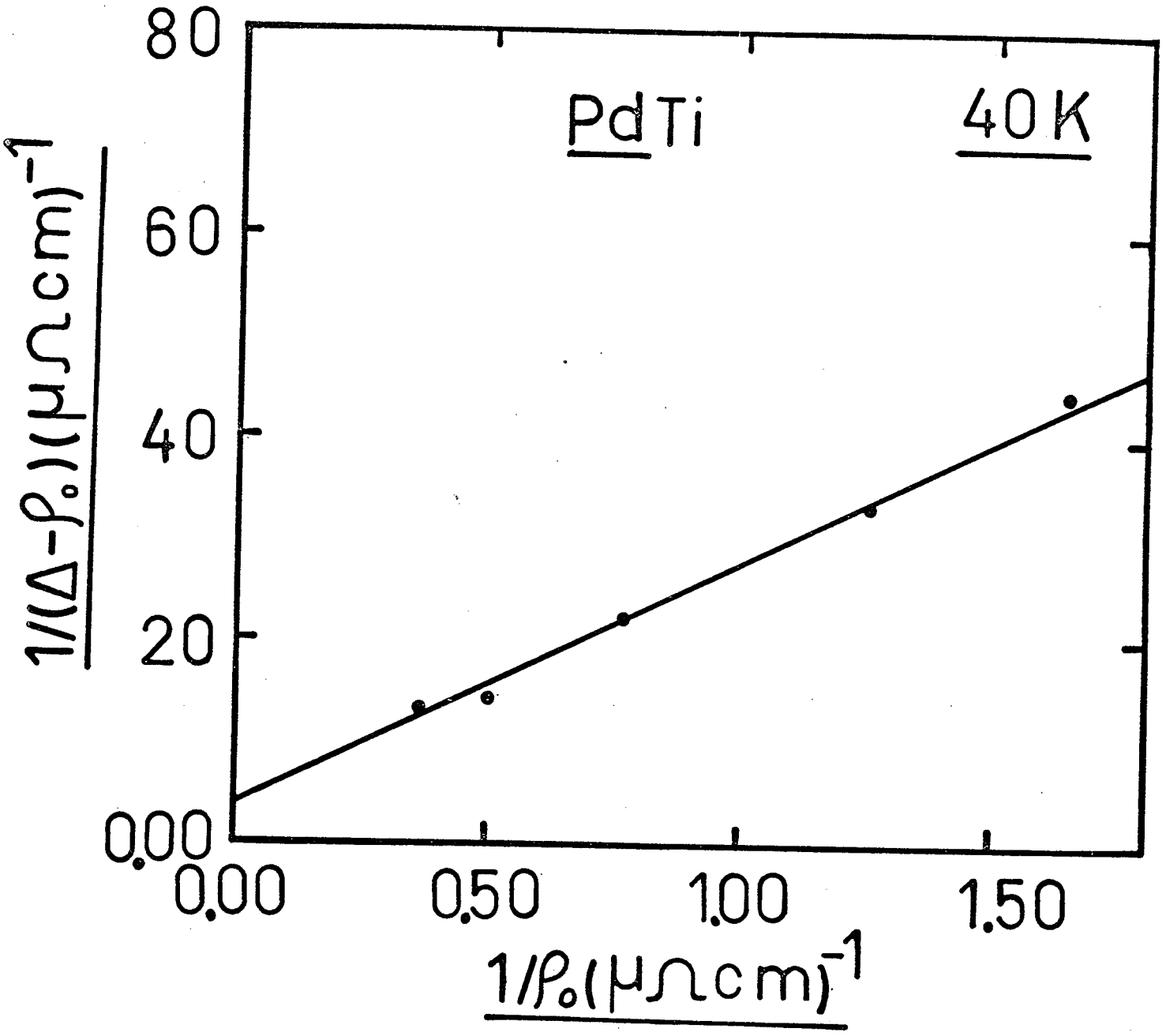

Fig. (3-17)

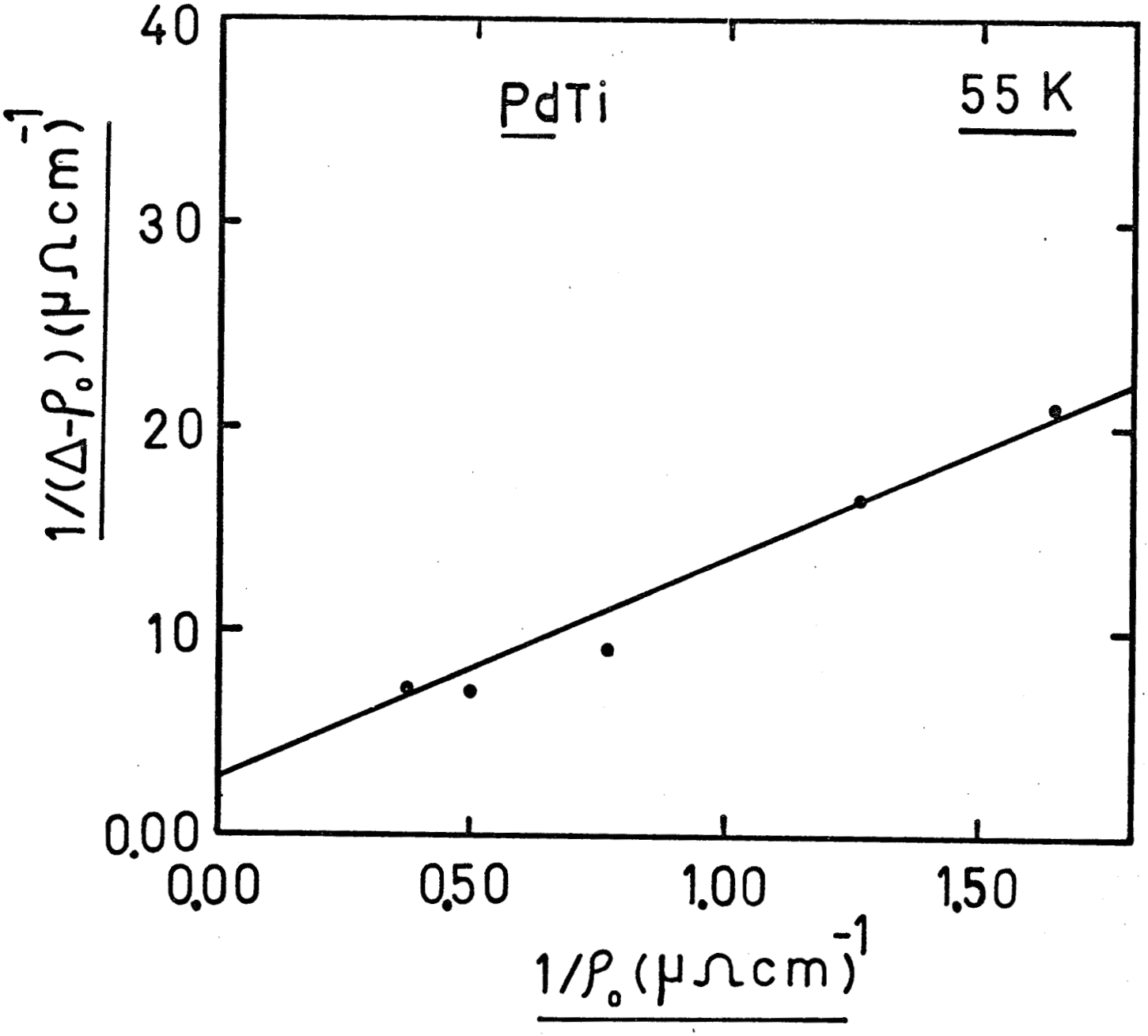

Fig. (3-18)

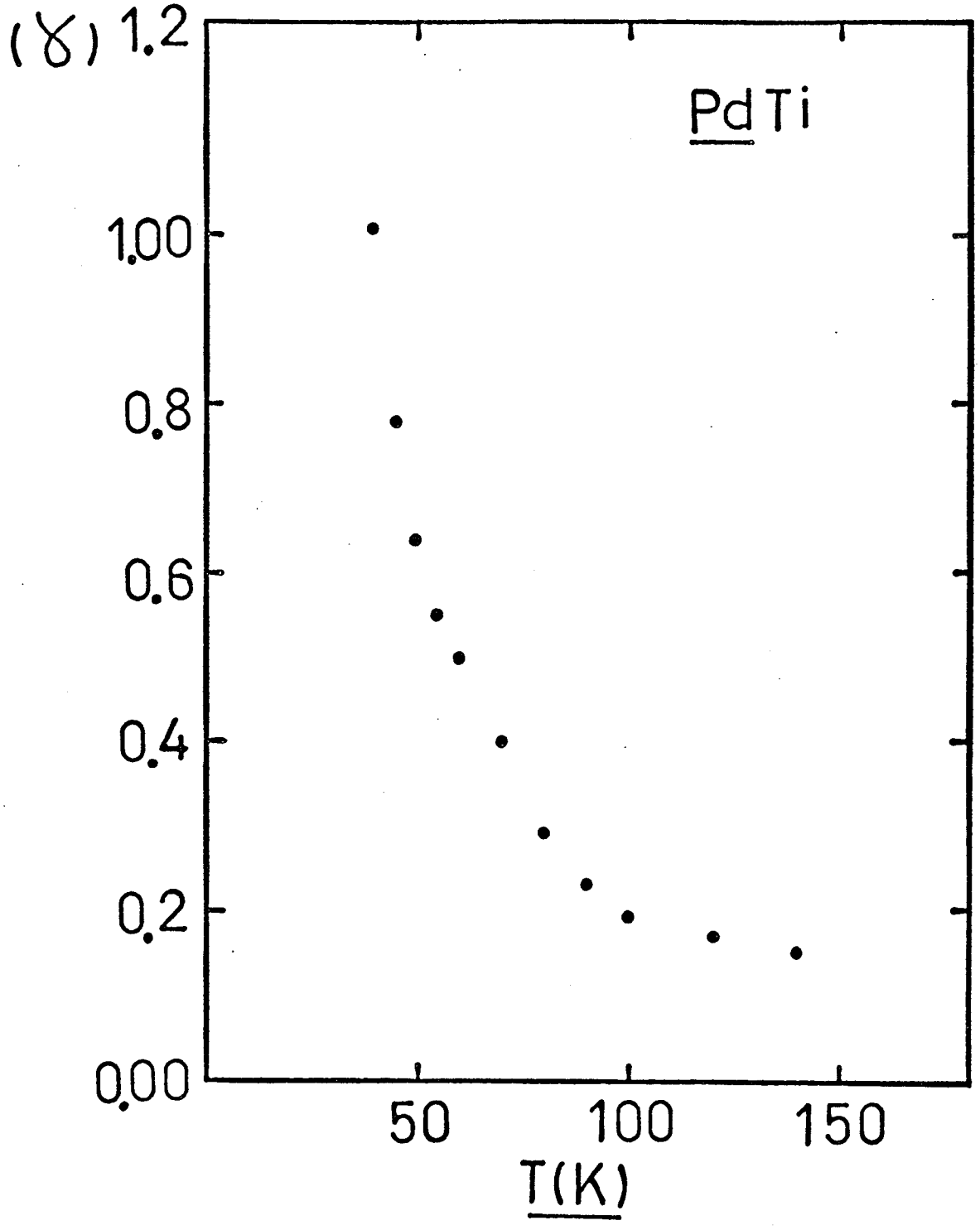

Fig. (3-19)

$$b \equiv (\beta - \gamma - \beta\gamma)^2/\gamma\beta^2 \qquad (3\text{-}15)$$

One sign in the above equations gives a value for $\alpha_p = \frac{\sigma_N}{\sigma_B}$ while the other sign gives the inverse value of the first one $\alpha_p = \frac{\sigma_B}{\sigma_N}$.

The values for α_p and α_i are shown in tables (3-2), (3-3), (3-4) and (3-5) for Pt Ti (two concentration) and Pt V and Pd Ti, respectively.

Due to Ziman[7], in the noble metals the belly electrons will have a relaxation time τ_B which will tend to increase rapidly at low temperatures since Umklapp Processes (which could cause wide angle scattering) will die out with falling temperature. On the other hand, the relaxation time of the neck electrons τ_N will not increase so rapidly because in the neck regions of the Fermi surface, the curvature is large and quite small phonons can still cause appreciable changes in the electron velocity. At high temperatures because of the large number of phonons with large wave number, scattering will be more or less isotropic.

i.e. $\frac{\tau_N}{\tau_B} \simeq 1$

Thus we expect $\frac{\tau_N}{\tau_B}$ to diminish as the temperature falls and becomes almost equal to one at high temperatures.

The larger α_p at high temperatures is interpreted in terms of a phonon scattering which becomes increasingly isotropic as the temperature increases.

The electronic band structure in Pt[8] and Pd[8] are more complicated than that in Au and we can not simply talk about belly and neck electrons in Pt and Pd alloys. However, similar conclusions

should hold in Pd and Pt at high temperatures when scattering in the two "bands" should be thermally randomized.

An interesting property of α_p in Pt V and Pt Ti alloys which we observed was that it has a smooth variation, in fact it increases with temperature toward a value of unity (this increase has been attributed to phonon scattering becoming increasingly isotropic as the temperature increases) and as the temperature is increased further, α_p starts decreasing and decreases continuously up to room temperature.

The change in sign of the temperature derivative of α_p and α_i which is a property of the two band model occurs in the region of transition from $\gamma > \beta$ to $\beta > \gamma$. This change will also occur in noble metal based alloys if the decrease in γ evident below 60K persists to higher temperatures.

Thus the phonon scattering which was assumed to become increasingly isotropic as the temperature increases, must now revert to becoming increasingly anisotropic as the temperature is increased still further. The physical basis for such an effect is not clear. This result casts further doubt on the physical basis of the two band model.

In Pd Ti alloys α_p is increasing with temperature above 40K and below 40K we can not get definite results because of the small deviations below 40K for these alloys. So, in Pt Ti and Pt V we can use constant β and temperature dependent γ, but in Pd Ti we had to let β and γ both be temperature dependent.

T	β
25	0.041
30	0.042
35	0.045
40	0.041
45	0.059
50	0.084
55	0.093
60	0.100
70	0.130
80	0.180
90	0.220
100	0.240
120	0.270
140	0.260
160	0.170

TABLE (3-1)

T	%	γ	α_p	α_i(taking + sign)	α_i(taking-sign)
15	0.25	2.0761	0.021	0.291	
20	0.25	0.7710	0.080	0.432	
25	0.25	0.4950	0.150	0.581	
30	0.25	0.4996	0.150	0.582	
35	0.25	0.3521	0.280	0.866	
40	0.25	0.2650	0.500	1.359	
45	0.25	0.2013	0.930	2.402	
50	0.25	0.1540	0.590		0.2217
60	0.25	0.0950	0.220		0.0659
70	0.25	0.0729	0.140		0.0352
80	0.25	0.0599	0.100		0.0210
90	0.25	0.0492	0.070		0.0110
100	0.25	0.0408	0.060		0.0097
120	0.25	0.0319	0.040		0.0044
140	0.25	0.0260	0.030		0.0023
160	0.25	0.0221	0.024		0.0019
180	0.25	0.0205	0.024		0.0018
200	0.25	0.0169	0.019		0.0011
220	0.25	0.0151	0.017		0.0009
240	0.25	0.0136	0.015		0.0007
260	0.25	0.0126	0.014		0.0007
280	0.25	0.0116	0.013		0.0006
300	0.25	0.0110	0.012		0.0005

TABLE (3-2)

T	%	γ	α_p	α_i(taking + sign)	α_i(taking-sign)
15	1.0	3.5087	0.01	0.272	
20	1.0	1.0530	0.05	0.360	
25	1.0	0.6825	0.09	0.449	
30	1.0	0.5459	0.13	0.538	
35	1.0	0.4081	0.21	0.711	
40	1.0	0.3476	0.29	0.889	
45	1.0	0.2985	0.39	1.111	
50	1.0	0.2482	0.58	1.546	
60	1.0	0.1743	0.78		0.300
70	1.0	0.1458	0.52		0.192
80	1.0	0.1259	0.38		0.133
90	1.0	0.1035	0.26		0.082
100	1.0	0.0879	0.19		0.053
120	1.0	0.0678	0.12		0.027
140	1.0	0.0556	0.09		0.018
160	1.0	0.0465	0.07		0.012
180	1.0	0.0432	0.06		0.009
200	1.0	0.0356	0.05		0.007
220	1.0	0.0318	0.04		0.004
240	1.0	0.0287	0.04		0.005
260	1.0	0.0265	0.03		0.002
280	1.0	0.0246	0.03		0.002
300	1.0	0.0234	0.02		0.002

TABLE (3-3)

T	%	γ	α_p	α_i(taking + sign)	α_i(taking - sign)
20	1.0	2.8170	0.01	0.252	
25	1.0	3.2460	0.01	0.246	
30	1.0	1.3360	0.03	0.288	
35	1.0	0.7632	0.06	0.352	
40	1.0	0.5670	0.10	0.443	
45	1.0	0.4911	0.13	0.510	
50	1.0	0.3902	0.19	0.635	
55	1.0	0.3439	0.24	0.740	
60	1.0	0.3023	0.31	0.888	
70	1.0	0.2401	0.51	1.324	
80	1.0	0.1794	0.99		0.400
90	1.0	0.1497	0.65		0.257
100	1.0	0.1277	0.45		0.169
120	1.0	0.0996	0.27		0.091
140	1.0	0.0826	0.19		0.057
160	1.0	0.0647	0.12		0.029
180	1.0	0.0583	0.10		0.022
200	1.0	0.0540	0.09		0.019
220	1.0	0.0510	0.08		0.015
240	1.0	0.0467	0.07		0.012
260	1.0	0.0443	0.07		0.013
280	1.0	0.0417	0.06		0.009
300	1.0	0.0398	0.06		0.010

TABLE (3-4)

T	γ	α_p	α_i(taking + sign)
25	0.433	0.004	0.0496
30	0.490	0.003	0.0498
35	0.491	0.004	0.0540
40	1.004	0.001	0.0446
45	0.780	0.004	0.0685
50	0.640	0.012	0.1090
55	0.550	0.018	0.1302
60	0.500	0.024	0.1490
70	0.400	0.060	0.2530
80	0.292	0.210	0.6100
90	0.230	0.570	1.4600
100	0.194	0.990	2.5450
120	0.170	1.610	4.4830
140	0.149	2.010	5.6640

TABLE (3-5)

References

1. W.J. deHaas and J. deBoer, Physica, 1, 609, (1934).
2. E. Krautz and H. Schultz, Z. Naturf. A, 12, 710, (1957).
3. P.G. Klemens and G.C. Lowenthal, Aust. J. Phys., 14, 352, (1961).
4. R.G. Stewart and R.P. Huebener, Phys. Rev., B1, 3323, (1970).
5. P. Alley and B. Serin, Phys. Rev., 116, 334, (1959).
6. G.K. White and S.B. Woods, Phil. Trans. Roy. Soc. London, A251, 273, (1959).
7. J.M. Ziman, Phys. Rev., 121, 1320, (1961).
8. O. Krogh Anderson, Phys. Rev., B2, 883, (1970).
9. T.E. Whall, P.J. Ford and J.W. Loram, Phys. Rev., B6, 3501, (1972).

Appendix 1

From the circuit in Fig. (1-2) we conclude:

$$\rho_{tot} = \frac{(\rho_B^{ph} + \rho_B^o)\ (\rho_N^{ph} + \rho_N^o)}{\rho_B^{ph} + \rho_B^o + \rho_N^{ph} + \rho_N^o}$$

By using:

$$\rho_N^{ph} = \frac{\rho_B^{ph}}{\alpha_p} \qquad \text{and} \qquad \rho_N^o = \frac{\rho_B^o}{\alpha_i}$$

we get:

$$\rho_{tot} = \frac{(\rho_B^{ph} + \rho_B^o)\ (\frac{\rho_B^{ph}}{\alpha_p} + \frac{\rho_B^o}{\alpha_i})}{\rho_B^{ph} + \rho_B^o + \frac{\rho_B^{ph}}{\alpha_p} + \frac{\rho_B^o}{\alpha_i}}$$

$$\rho_{ph} = \frac{\rho_N^{ph}\ \rho_B^{ph}}{\rho_N^{ph} + \rho_B^{ph}} = \frac{\frac{\rho_B^{ph}}{\alpha_p}\ \rho_B^{ph}}{\frac{\rho_B^{ph}}{\alpha_p} + \rho_B^{ph}} = \frac{\rho_B^{ph}}{\alpha_p + 1}$$

$$\rho_o = \frac{\rho_B^o}{\alpha_i + 1}$$

$$\rho_{tot} = \frac{[(\alpha_p + 1)\rho_{ph} + \rho_o(\alpha_i + 1)][\alpha_i\ \rho_{ph}(\alpha_p + 1) + \alpha_p\ \rho_o(\alpha_i + 1)]}{\alpha_p\alpha_i\ \rho_{ph}(\alpha_p + 1) + \alpha_p\alpha_i\ \rho_o(\alpha_i + 1) + \alpha_i\ \rho_{ph}(\alpha_p + 1) + \alpha_p\rho_o(\alpha_i + 1)}$$

$$\rho_{tot} = \frac{\alpha_i(\alpha_p + 1)^2\ \rho_{ph}^2 + (\alpha_p + 1)(\alpha_i + 1)\rho_o\ \rho_{ph}(\alpha_p + \alpha_i) + \alpha_p\ \rho_o^2(\alpha_i + 1)^2}{\alpha_i\ \rho_{ph}(\alpha_p + 1)^2 + \alpha_p\ \rho_o(\alpha_i + 1)^2}$$

But:

$$\Delta(C,T) = \rho_{tot} - \rho_{ph} - \rho_o$$

which yields;

$$\Delta(C,T) = \frac{\rho_o \rho_{ph}(\alpha_i - \alpha_p)^2}{\alpha_p \rho_o(1 + \alpha_i)^2 + \alpha_i \rho_{ph}(1 + \alpha_p)^2}$$

By dividing numerator and denominator by $(\alpha_i - \alpha_p)^2$ we get:

$$\Delta(C,T) = \frac{\rho_o \rho_{ph}}{\rho_o \frac{\alpha_p(1 + \alpha_i)^2}{(\alpha_p - \alpha_i)^2} + \rho_{ph} \frac{\alpha_i(1 + \alpha_p)^2}{(\alpha_p - \alpha_i)^2}}$$

we call:

$$\gamma = \frac{1}{\alpha_p} \left(\frac{\alpha_p - \alpha_i}{1 + \alpha_i}\right)^2$$

and

$$\beta = \frac{1}{\alpha_i} \left(\frac{\alpha_p - \alpha_i}{1 + \alpha_p}\right)^2$$

so we get:

$$\Delta(C,T) = \frac{\gamma\beta \rho_o \rho_{ph}}{\gamma \rho_{ph} + \beta\rho_o}$$

and

$$\frac{1}{\Delta(C,T)} = \frac{1}{\beta \rho_o} + \frac{1}{\gamma \rho_{ph}}$$